Resource

Structure

Conformational Chaperones for Structural Studies of Membrane Proteins Using Antibody Phage Display with Nanodiscs

Graphical Abstract

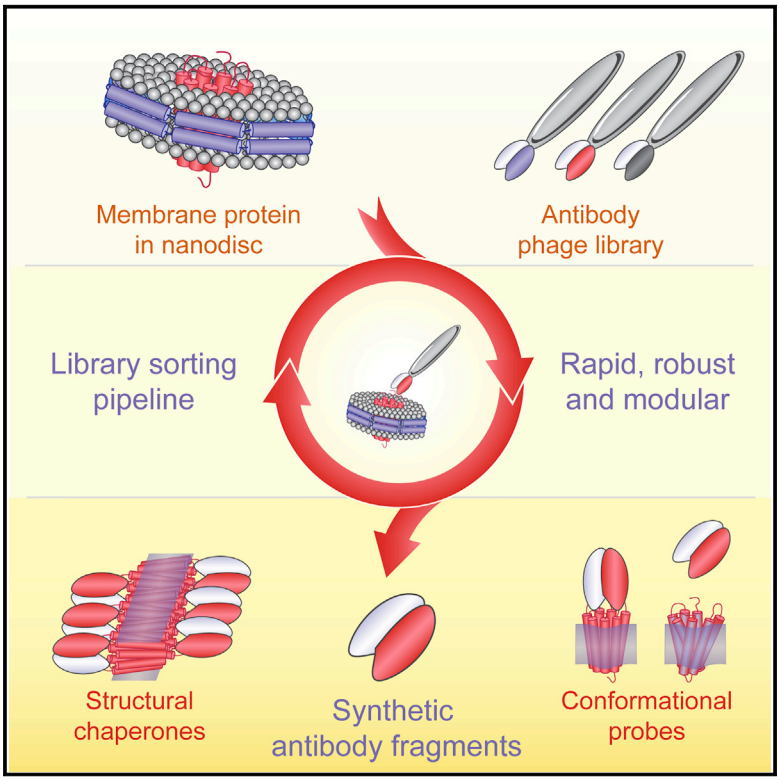

Authors

Pawel K. Dominik, Marta T. Borowska, Olivier Dalmas, Sangwoo S. Kim, Eduardo Perozo, Robert J. Keenan, Anthony A. Kossiakoff

Correspondence

koss@bsd.uchicago.edu

In Brief

Generation of affinity reagents for structural and functional characterization of membrane proteins is challenging in detergents. Dominik et al. describe an improved antibody phage display protocol for membrane proteins exploiting nanodiscs. This expands the usability of the method to multiple challenging membrane protein systems.

Highlights

- Nanodiscs allow for generation of multiple antibody fragments to membrane proteins
- Improved phage display protocol is fast, efficient, and modular
- Resulting antibodies probe protein conformations present in lipid environment
- Expands the toolbox for structural and functional studies of membrane proteins

Dominik et al., 2016, Structure *24*, 300–309
February 2, 2016
http://dx.doi.org/10.1016/j.str.2015.11.014

CellPress

Structure
Resource

Conformational Chaperones for Structural Studies of Membrane Proteins Using Antibody Phage Display with Nanodiscs

Pawel K. Dominik,[1] Marta T. Borowska,[1] Olivier Dalmas,[1,2] Sangwoo S. Kim,[1] Eduardo Perozo,[1] Robert J. Keenan,[1] and Anthony A. Kossiakoff[1,*]
[1]Department of Biochemistry and Molecular Biology, The University of Chicago, 929 East 57th Street, Chicago, IL 60637, USA
[2]Present address: NGM Biopharmaceuticals, Inc., 630 Gateway Boulevard, South San Francisco, CA 94080, USA
*Correspondence: koss@bsd.uchicago.edu
http://dx.doi.org/10.1016/j.str.2015.11.014

SUMMARY

A major challenge in membrane biophysics is to define the mechanistic linkages between a protein's conformational transitions and its function. We describe a novel approach to stabilize transient functional states of membrane proteins in native-like lipid environments allowing for their structural and biochemical characterization. This is accomplished by combining the power of antibody Fab-based phage display selection with the benefits of embedding membrane protein targets in lipid-filled nanodiscs. In addition to providing a stabilizing lipid environment, nanodiscs afford significant technical advantages over detergent-based formats. This enables the production of a rich pool of high-performance Fab binders that can be used as crystallization chaperones, as fiducial markers for single-particle cryoelectron microscopy, and as probes of different conformational states. Moreover, nanodisc-generated Fabs can be used to identify detergents that best mimic native membrane environments for use in biophysical studies.

INTRODUCTION

Membrane proteins represent a class of proteins whose known functions are governed by sets of programmed conformational transitions induced by a broad spectrum of external stimuli. Establishing the linkages between structure, function, and dynamics has proved extremely challenging due to a lack of tools and approaches that can provide qualitative information to accurately describe the dynamic energy landscapes that underlie membrane protein functions. While biophysical and computational analyses contribute to this endeavor, the key element in establishing these linkages is to start from the high-resolution structures of the functionally relevant conformational states of the protein.

The underlying problem in obtaining this structural information is that the lifetime of many mechanistically important conformations of membrane proteins are often too fleeting to be studied by time-averaged techniques such as crystallography or single-particle cryoelectron microscopy (cryo-EM). Attempts to stabilize intermediate states through mutagenesis or by adding ligands or ions have been only marginally successful. Thus, new strategies are required that are able to capture and stabilize the protein's mechanistically important conformational states. To address these technical challenges, we have developed a technology platform that overcomes the main roadblocks that had previously frustrated attempts to acquire the types of structural information needed to link dynamics with function. A central component of this platform is a phage display pipeline that has the capacity to generate high-performance antibody-based reagents that are exquisitely conformation selective. As such, they can effectively "capture" a protein in a desired conformational form, allowing for unequivocal annotation of distinct functional states through biophysical analyses and structure determination. The phage display libraries, built upon well-characterized Fab scaffolds, are fully synthetic and, thus, the generated reagents are termed "synthetic antibodies" or sABs (Fellouse et al., 2007). In addition to stabilizing desired conformational states, Fabs have also proved extremely powerful as crystallization chaperones and fiducial markers for single-particle cryo-EM to aid in the structure determination of these states (Wu et al., 2012; Bukowska and Grutter, 2013).

The methodologies for generating conformationally selective sABs for complex soluble proteins including multi-domain and transient multi-protein systems have been established (Rizk et al., 2011; Paduch et al., 2013; Mateja et al., 2015). These methods with several modifications have also proved successful for phage display selections to generate sABs to membrane proteins in detergent (Uysal et al., 2009; Kim et al., 2011; Li et al., 2014). However, our experience has shown that for membrane proteins, the process is not straightforward and the required adaptations are system dependent (Dominik and Kossiakoff, 2015). In particular, in many cases membrane protein stability is compromised by the detergent, resulting in structural heterogeneity that confounds the generation of sAB binders to a single conformational state (A.A.K., unpublished data). Moreover, it is generally acknowledged that detergents can introduce their own conformational biases, which many times are incompatible with native conformations in the membrane environment (Sonoda et al., 2011; Chung et al., 2012). Finally, in some cases we encounter the difficulty of biotinylating detergent-solubilized membrane proteins, which is required for efficient phage library

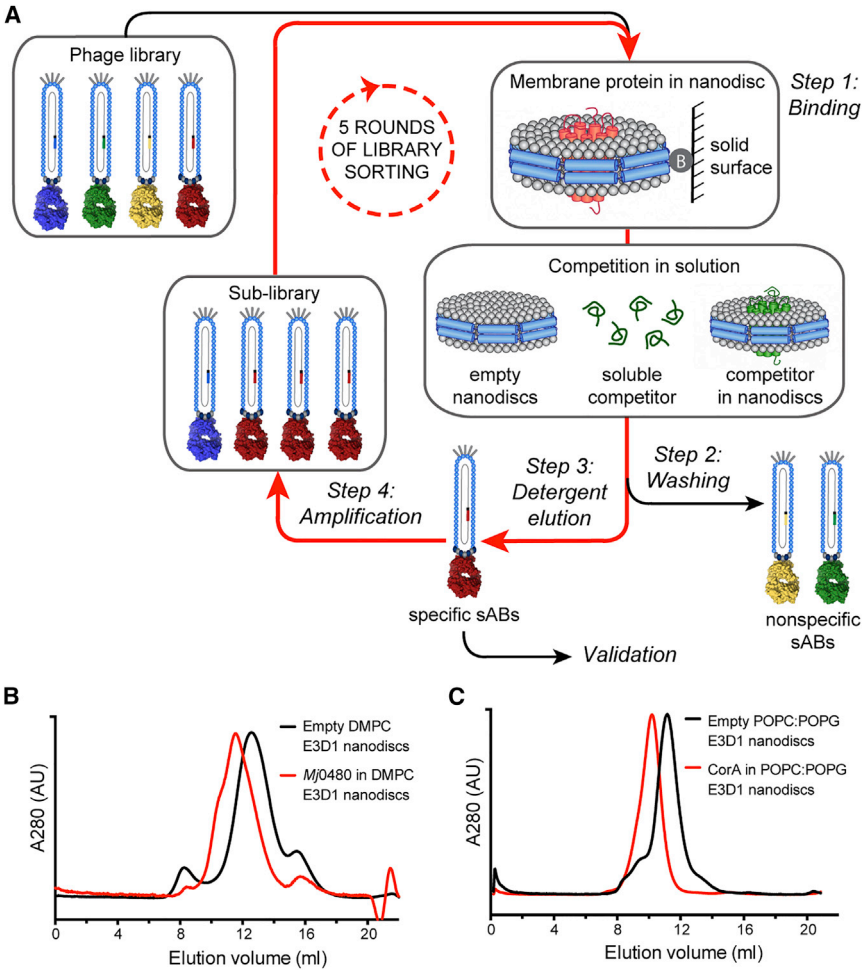

Figure 1. Antibody Phage Display with Membrane Proteins in Nanodiscs

(A) Sequence of phage display sorting steps: (1) incubation of the nanodisc-embedded protein target with phage display library and competitors; (2) washing step to remove weak and non-specific binders; (3) detergent elution of protein and specific phage particles; (4) amplification of specific binders in *E. coli*. The cycle is repeated increasing the stringency by decreasing the concentration of the target. Usually high-quality synthetic antibodies (sABs) are obtained in four to five cycles.

(B and C) Size-exclusion chromatography profiles upon reconstitution of *Mj*0480 (B, in red) and CorA (C, in red) when compared with empty nanodisc controls (B and C, in black). AU, arbitrary units. See also Figure S1.

sorting steps on a solid support and introduces additional optimization steps.

We sought to address these limitations by embedding the membrane proteins in lipid-filled nanodiscs during the phage display generation of sAB binders. Nanodiscs are discoidal particles composed of a lipid bilayer surrounded by a belt comprising two copies of an amphipathic α-helical protein called a membrane scaffold protein (MSP) (Ritchie et al., 2009; Bayburt and Sligar, 2010). Nanodiscs have been used in structural and functional studies of membrane proteins of various architectures (Bayburt and Sligar, 2010). For the purposes of antibody phage display, nanodiscs allow the protein targets to be reconstituted into a native-like lipid environment with access to the protein from both sides of the membrane, and enable the user to bypass difficulties in sample handling, thus increasing the overall stability of the antigen (Bayburt et al., 2006). The diameter and chemical makeup of nanodiscs can be adjusted during protein reconstitution by using different variants of MSP and various lipid compositions (Ritchie et al., 2009; Hagn et al., 2013). Importantly, any modifications of the antigens necessary for the phage display experiment, such as biotinylation, can be readily achieved by attachment through MSP or lipid modifications, leaving the membrane protein unaltered. Further, sABs derived from nanodisc selections can be used to profile a battery of different detergents to accurately assess how compatible each is with preserving the native conformational states of a membrane protein compared with the lipid-like environment. Thus, taken together, embedding membrane protein targets into nanodiscs is a natural progression of antibody phage display technology performed outside of detergent environments.

To optimize the use of nanodiscs in the phage display selection pipeline and assess the resulting advantages, we employed two membrane protein systems possessing different architectures: a small YidC homolog from *Methanocaldococcus jannaschii*, *Mj*0480, and a pentameric magnesium ion channel from *Thermotoga maritima*, CorA. We show that this modified pipeline is capable of generating robust crystallization chaperones as well as conformation-specific sABs. In parallel, we compare the nanodisc protocol with the standard, detergent-based sorting strategy, and characterize the influence of the membrane protein lipid environment on the apparent affinity of sABs for their cognate antigen. We also systematically assess the compatibility of each sAB with detergents commonly used in structure determination. These types of customized sABs generated for targets in nanodiscs will provide membrane protein biologists with new tools that have broad application both inside and outside the structural biology community.

RESULTS

Modifications to the Phage Display Sorting Strategy

The phage display sorting procedure performed to generate the sABs (Figure 1A) is based on a previously described solution capture scheme utilizing a Kingfisher magnetic beads handler (Fellouse et al., 2007; Paduch et al., 2013; Dominik and Kossiakoff, 2015). Membrane proteins were reconstituted into nanodiscs (Figures 1B and 1C) after optimization following established

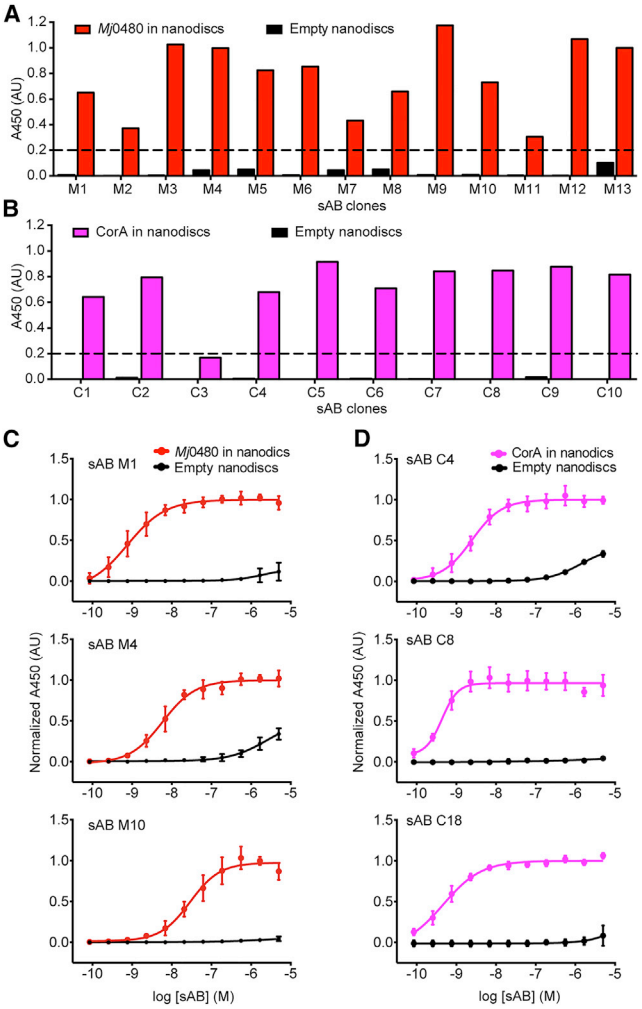

Figure 2. Initial Validation of sABs against *Mj*0480 and CorA Generated from Library Sorting in Nanodiscs

(A and B) ELISA binding signal of sABs in phage format generated against *Mj*0480 (A) and CorA (B) after five rounds of library sorting with nanodiscs. The high binding signal of sAB-phage particles is observed only for *Mj*0480 in eggPC E3D1 nanodiscs (red), or CorA in POPC/POPG E3D1 nanodiscs (magenta), but not for empty nanodiscs (black). Dotted horizontal lines represents four times the average background level.

(C and D) EC_{50} evaluation of apparent binding affinities of sABs in protein format generated against *Mj*0480 (C) and CorA (D). In all cases, sABs show low nanomolar apparent binding affinity to *Mj*0480 in nanodiscs (C, red) or CorA in nanodiscs (D, magenta), but not to empty nanodiscs (black). Data points in (C) and (D) show average values from three independent experiments in triplicates. Error bars display SD value from the mean.

See also Figure S2.

protocols (Ritchie et al., 2009; Bayburt and Sligar, 2010). The diameter of the nanodisc can be adjusted to accommodate different size target proteins or oligomeric states using different variants of the MSP (Bayburt et al., 2006). Both *Mj*0480 and CorA were embedded in ~12-nm nanodiscs produced from an MSP E3D1 variant. Note, however, that the size of the disc is not overly critical as long as it is large enough to provide sufficient room to accommodate several layers of lipid between the protein and the MSP.

Table 1. EC_{50} Values of sABs Generated against *Mj*0480 in Library Sorting Experiments Performed in Nanodiscs and DDM

	EC_{50} Apparent Binding Affinity (nM)			
sAB	*Mj*0480 in Nanodiscs	*Mj*0480 in DDM	*Mj*0480 in FC-12	Empty Nanodiscs
Generated in nanodiscs				
M1	<1	>1,000	<1	no binding
M3	3 ± 0.5	2.5 ± 1	2 ± 0.5	700 ± 100
M4	6 ± 1.5	2.5 ± 0.5	2 ± 0.5	>1,000
M10	30 ± 7	45 ± 10	10 ± 1.5	no binding
M22	<1	100 ± 30	<1	>1,000
M29	16 ± 4	(~500)[a]	620 ± 20	no binding
Generated in DDM				
F1	700 ± 100	200 ± 100	70 ± 35	1,000 ± 240
F2	18 ± 5.5	54 ± 6	20 ± 2	400 ± 50
F3	14 ± 3	40 ± 11	12 ± 2	160 ± 30
F4	63 ± 11	130 ± 19	24 ± 6	87 ± 12
F5	61 ± 4	5 ± 0.5	2.5 ± 1	210 ± 15
F7	810 ± 170	320 ± 50	165 ± 40	>1,000

[a]Value ambiguous.

Efficient phage display sorting requires reversible and controllable immobilization to pull down the protein-loaded nanodiscs; this is typically achieved by direct biotinylation of the target, which is then captured on streptavidin beads. By chemically biotinylating MSP or introducing a genetic Avi-tag into MSP, the need for direct biotinylation of the detergent-solubilized membrane proteins, which often destabilizes the target, is eliminated. Moreover, this strategy enhances epitope accessibility by providing equal access to both sides of the protein's surface in comparison with cases where protein modification is preferential to one side of the membrane. Simple pull-down experiments using streptavidin-coated magnetic beads were used to test the immobilization efficiency of the biotinylated E3D1 nanodiscs. In general, we achieved more than 90% efficiency of immobilization and elution of nanodiscs containing both tested membrane proteins (Figures S1A and S1B), which is within the desired range of immobilization required for successful library sorting. Conveniently, disassembly of the nanodiscs and release of the membrane protein (and bound phage) was achieved by short incubation of the magnetic beads with detergent.

Generating High-Affinity sABs

To assess the overall performance of the modified protocol in nanodiscs, we carried out five rounds of sorting on the two model systems: *Mj*0480 and CorA. During rounds 1–5, the protein-nanodisc target concentration was decreased incrementally from around 200–400 nM to a 10–30 nM range (Table S1). In addition, a 5- to 10-fold molar excess of empty non-biotinylated E3D1 nanodiscs was added as soluble competitors starting from round 2. This strategy eliminates most of the nanodisc- and lipid-specific binders. The sorting progress was monitored by comparing enrichment of the eluted phage particles after each round. Enrichment is a measure of the number of target-specific phage particles that are isolated after a particular round compared with background. As a rule, we generally observe

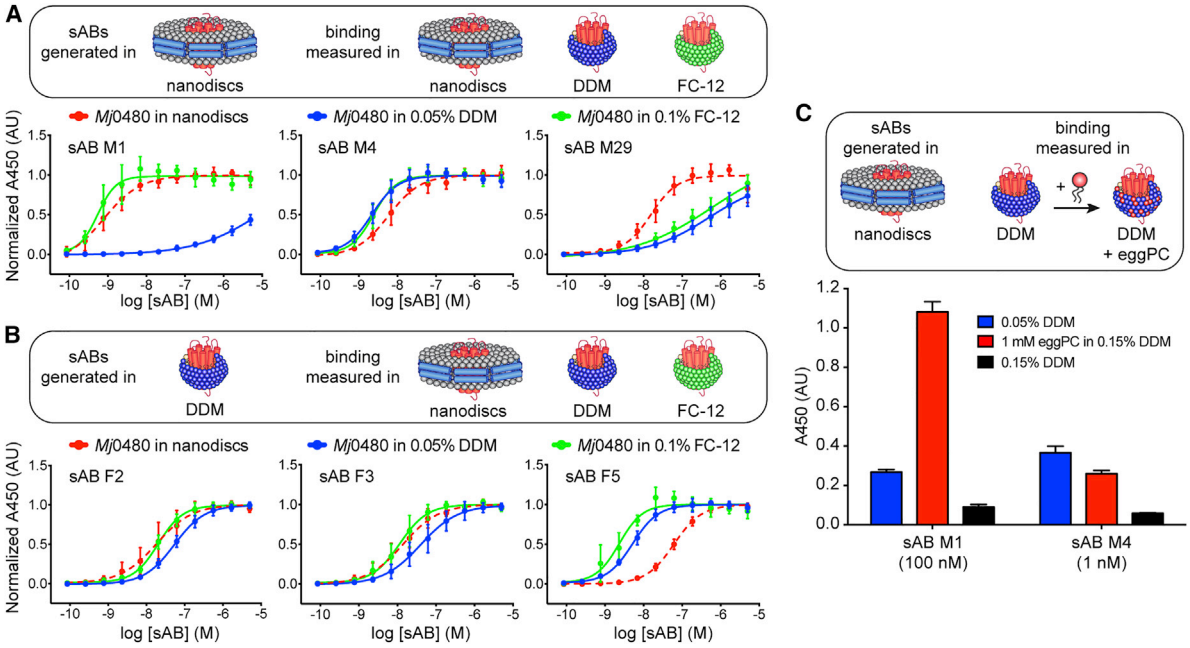

Figure 3. Effect of Detergents on Binding Affinity of *Mj*0480 sABs Generated in Nanodiscs and DDM

(A and B) EC_{50} evaluation of apparent binding affinity of *Mj*0480 sABs generated against the antigen in nanodiscs (A) and DDM (B). All sABs in protein format were tested for binding with biotinylated *Mj*0480 in 0.05% DDM (blue, solid), 0.1% FC-12 (green, solid), or *Mj*0480 in biotinylated eggPC E3D1 nanodiscs (red, dashed). (C) Single-point protein ELISA of binding of sABs M1 and M4 to biotinylated *Mj*0480 in DDM in the absence (blue and black) or presence of eggPC phospholipids solubilized in DDM (red). Concentration of sABs M1 and M4 used in the experiment was below established EC_{50} values of binding in DDM and was 100 and 1 nM, respectively.

Data points show average values from three independent experiments in triplicates. Error bars display SD value from the mean. See also Figures S3 and S4.

10- to 100-fold enrichment after the final round; however, successful results have been obtained with lower (and higher) levels of enrichment (data not shown). In both cases here, we observed enrichment in the expected range comparing phage particles eluted from the sample to background values determined using empty nanodiscs or streptavidin beads only (Figure S1C).

To evaluate the affinity and specificity of the sAB clones obtained after library sorting, we picked approximately 48 clones from each selection. After amplification in *Escherichia coli*, initial binding properties were determined by single-point phage ELISA. Clones with an ELISA signal higher than four times the average background level were sequenced. A total of 14 and 10 unique sABs were obtained from the library sorting against *Mj*0480 and CorA, respectively (Figures 2A, 2B, and S2). Next, we expressed three sABs from each set and measured their apparent binding affinity against target-embedded nanodiscs by multi-point protein ELISA (EC_{50}) (Figures 2C and 2D). All tested sABs had nanomolar affinities for their respective targets in nanodiscs, and virtually no affinity to empty nanodiscs. Thus, the use of nanodisc-embedded membrane proteins during phage display facilitates generation of multiple specific sABs with high affinity toward the targets of interest.

Comparison of Nanodisc- and Detergent-Based Sorting Protocols

A side-by-side comparison of the phage display sorting protocols in nanodiscs and detergent was performed. After five rounds of sorting using *Mj*0480 as the target, we obtained 12 unique sAB clones from the nanodisc format and seven from the detergent (dodecyl maltoside [DDM]) format (Figure S2). To test for detergent effects on sABs binding to their cognate protein targets, we selected six sABs generated for *Mj*0480 in nanodiscs (sABs M1, M3, M4, M10, M22, and M29) and six sABs from library sorting in DDM (sABs F1–F5 and F7). When measured in the environment in which the respective library sorting experiments were performed (i.e., nanodisc or detergent), the nanodisc selected sABs all had affinities <30 nM; in contrast, the DDM sABs had affinities ranging from 5 to 300 nM (Table 1). While a number of the sABs bind to nanodisc-embedded target regardless of the medium from which they were generated (Figures 3A and 3B), many are biased toward the initial format used during library sorting (e.g., sABs M1 and M29, for nanodiscs, and sABs F5 and F7, for DDM). This suggests that at least some sABs are sensitive to the initial setup of library sorting experiments (nanodiscs or DDM).

Using sABs generated to *Mj*0480, six obtained from the selections in the nanodiscs and six from DDM, we next compared the EC_{50} binding values of these sABs against the target in nanodisc format and two different detergents: DDM and fos-choline-12 (FC-12) (Figures 3A, 3B, and S3). These comparisons showed that some of the sABs displayed significant detergent sensitivity. In general, for nanodisc-generated sABs, binding in FC-12 tracks better with binding in nanodiscs than binding in DDM (especially visible for sABs M1 and M22). This can be attributed to several factors: differences in the protein's conformation in different detergents, similarity in chemical makeup of FC-12

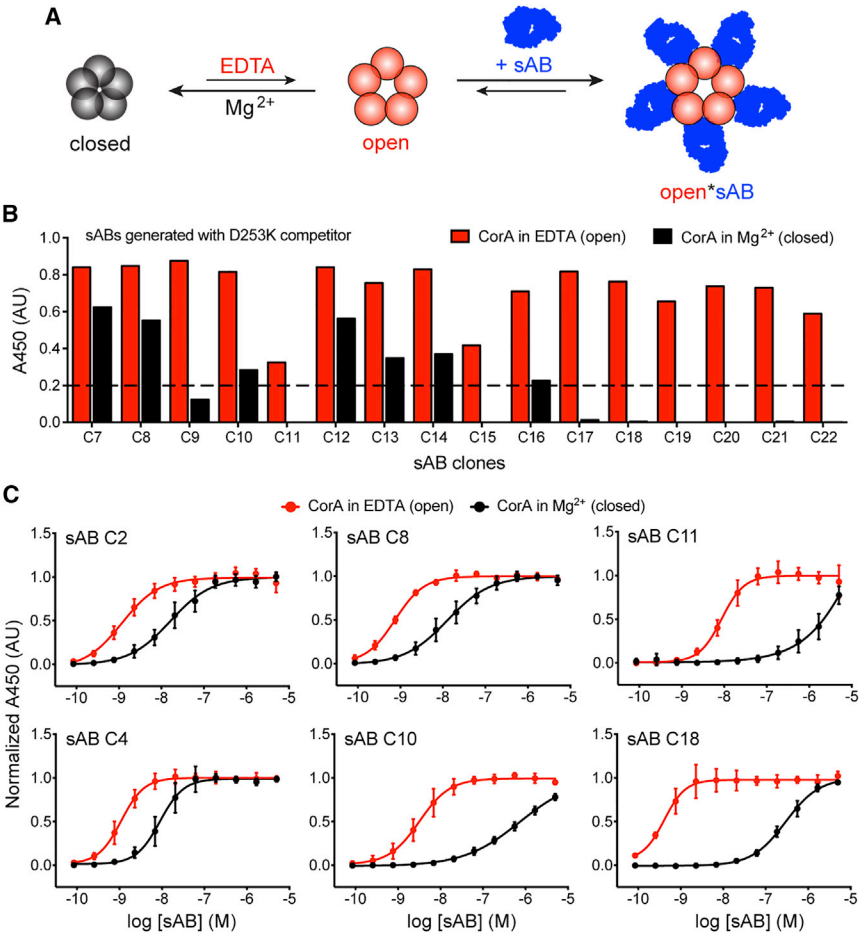

Figure 4. Conformation-Specific sABs of CorA

(A) Schematic representation of the conformational transition of the pentameric magnesium ion channel, CorA. In the presence of Mg^{2+} ions CorA collapses to stable closed state (black); removal of Mg^{2+} with EDTA triggers opening of the channel (red). A desirable open conformation-specific sAB (blue) would preferentially stabilize the open state of the channel.

(B) Representative binding signal of sABs C7–C22 in phage format, generated against CorA wild-type after five rounds of library sorting with CorA D253K competitor in nanodiscs. Multiple sABs show high binding signal for biotinylated CorA in nanodiscs in the presence of 1 mM EDTA (open state, red) versus 20 mM $MgCl_2$ (closed state, black). Dotted horizontal line represents four times the average background level.

(C) EC_{50} evaluation of apparent binding affinities of CorA sABs generated in the absence (sABs C2, C4, C8, and C10) or presence of D253K competitor in nanodiscs (sABs C8, C10, C11, and C18). sAB C8 and C10 were produced in both selection schemes. All shown sABs in protein format were tested for binding with biotinylated CorA in 0.05% DDM in the presence of 1 mM EDTA (open state, red) versus 20 mM $MgCl_2$ (closed state, black). Data points in show average values from three independent experiments in triplicates. Error bars display SD value from the mean.

See also Figure S5.

and phospholipids, or epitope availability caused by the smaller micelle size of FC-12 relative to DDM. This is not true for sABs C29 and F5 in which FC-12 binding tracks better with DDM binding, but is different in nanodiscs, suggesting differences in epitopes between both detergents and nanodisc formats.

A pertinent example of detergent effects is the nanodisc-generated sAB M1, which binds tightly to *Mj*0480 in both nanodiscs (K_d < 1 nM) and FC-12 (K_d < 1 nM), but significantly worse in DDM (K_d > 1,000 nM) (Figure 3A). Strikingly, binding of sAB M1 is restored in DDM when *Mj*0480 is pre-incubated with the lipids (including egg phosphatidylcholine [eggPC]) used for the nanodisc reconstitution (Figure 3C). Importantly, this effect is not seen for another nanodisc-generated sAB (M4), which has a similar affinity (K_d ~2–6 nM) to *Mj*0480 in nanodiscs, FC-12, and DDM (Figure 3C). Thus, in cases where sAB affinity is compromised by detergents, target binding can be at least partially restored by pre-incubating the protein in a small amount of lipid before detergent solubilization.

Finally, we compared the non-specific binding of sABs generated by each format. Compared with nanodisc-generated sABs, the detergent-generated sABs showed significantly higher background binding to empty nanodiscs (Figure S4). This suggests that the affinity of some detergent-generated sABs possesses a significant non-specific component that is not observed with the nanodisc-generated sABs. We attribute this to the possibility that during library sorting in detergent, there were no hydrophobic competitors similar to those provided by the lipid component of empty nanodiscs used in the counter selections as part of the nanodisc selection protocol. Importantly, comparing EC_{50} values for nanodisc-generated sABs in different detergents provides additional beneficial information on which detergents are most compatible to the native-like lipid environment.

Generation of Conformation-Specific sABs by Competitive Sorting in Nanodiscs

The ability to capture and stabilize a transient conformational state has many structural and biophysical applications, and we expected that the nanodisc strategy would be useful for generation of conformation-specific sABs in a native-like lipid environment. The well-characterized, homo-pentameric magnesium ion channel CorA from *T. maritima* reverts to a stable, closed (Mg^{2+}-bound) state in the presence of magnesium (Niegowski and Eshaghi, 2007; Moomaw and Maguire, 2008; Dalmas et al., 2014), and there are several structures of this form of the channel (Eshaghi et al., 2006; Lunin et al., 2006; Payandeh and Pai, 2006). However, attempts to obtain structural information about the open (Mg^{2+}-free), conductive state of the channel have been hampered by the flexibility of the metal-free protein (Dalmas et al., 2010, 2014; Pfoh et al., 2012). Thus, we designed

Table 2. EC_{50} Values of sABs Generated against CorA in Library Sorting Experiments Performed in Nanodiscs in the Absence or Presence of CorA D253K Competitor

	EC_{50} Apparent Binding Affinity (nM)				
sAB	CorA in Nanodiscs	Empty Nanodiscs	CorA in DDM/EDTA (Open)	CorA in DDM/Mg^{2+} (Closed)	EC_{50} Closed/ Open
Generated without D253K competitor					
C2	<1	ND[a]	1.5 ± 0.5	16 ± 4	11 ± 1
C4	2.5 ± 0.5	>1,000	1 ± 0.5	9 ± 2	11 ± 3.5
Generated without and with D253K competitor					
C8	<1	ND	<1	13 ± 3	(~20)[b]
C10	<1	ND	3 ± 0.5	75 ± 28	24.5 ± 5.5
Generated with D253K competitor					
C11	21 ± 5	ND	10 ± 1.5	>1,000	>100
C13	31 ± 3	ND	20 ± 2	>1,000	>50
C18	<1	ND	<1	300 ± 30	(>700)[b]

[a]No binding detected.
[b]Roughly approximated value.

nanodisc selections to generate sABs specific to the open Mg^{2+}-free CorA conformation.

Starting with phage clones collected after the first round of sorting against nanodisc-embedded CorA in which we generated ten CorA-specific sABs (C1–C10, Figures 2B and S2), we added 1 mM EDTA (to remove excess of magnesium ions) and 10-fold molar excess of a nanodisc-embedded CorA variant (D253K) in subsequent rounds (2 through 5). Although EDTA promotes the open form (Dalmas et al., 2014) it does not, by itself, eliminate the selection of sAB variants that bind to both states. In contrast, the CorA-D253K mutant is constitutively closed, even in the absence of magnesium (Payandeh et al., 2008); thus, we used it as soluble competitor to scavenge phage that binds preferentially to the closed conformation or indiscriminately to both the open and closed state of CorA.

Using this strategy, we generated 16 "open-state" specific sABs (C7–C22) (Figure S2). The affinities of these sABs for CorA were then tested in the presence of either 1 mM EDTA or 20 mM $MgCl_2$, which promote the channel in the open and closed state, respectively (Dalmas et al., 2014). Strikingly, each of the sABs showed a preference for the open conformation of CorA, with the specificity difference being higher for sABs obtained from selections with the D253K competitor (Figures 4B and S5B).

To better quantify the ability of the generated sABs to discriminate between the open and closed forms of the CorA channel and compare these characteristics between the selections with and without the D253K competitor, we expressed and purified these sABs (including those that were not put under D253K selection pressure). Almost all of these sABs had affinities <30 nM as measured by EC_{50} ELISA. From this set, six representative examples were picked from three types of library sorting categories: (1) EDTA only, (2) EDTA + D253K competitor, and (3) sABs that appeared in both categories (Figures 4C and S5B; Table 2). Again, all six showed significantly tighter binding toward CorA in EDTA (open) than in Mg^{2+} (closed). While the EDTA-selected sABs showed approximately 10-fold selectivity for the open versus closed state, for those sABs obtained in the sorting where the D253K was used the ratio was 100- to 700-fold higher, favoring the open state. The sABs that were identified in both selections (C7–C10) manifested properties intermediate to the two formats (~20- to 25-fold tighter to the open state). From these data, we conclude that the developed protocols performed with CorA in nanodiscs are effective in establishing sorting pressure geared toward conformational specificity when specific cofactors and soluble competitors in nanodiscs are added to push the equilibrium toward the desired protein state.

Nanodisc-Generated sABs as Crystallization Chaperones

*Mj*0480 has a relatively small solvent-exposed surface area and was recalcitrant to crystallization even after extensive effort (Borowska et al., 2015). To evaluate whether sABs generated from the nanodisc library sorting could be used as crystallization chaperones for detergent-solubilized proteins, we attempted purification of eight sAB-*Mj*0480 complexes in DDM by size-exclusion chromatography. In several cases, including sAB M1, which binds weakly to *Mj*0480 in DDM (Figure 3A), we observed stable complex formation on the column when molar excess of the sAB was incubated with the protein in DDM. After initial high-throughput screening, we obtained crystals for four sAB-*Mj*0480 complexes in DDM. Optimization of one of the conditions (sAB M1-*Mj*0480) (Figures 5A and 5B) ultimately yielded crystals that were solved to 3.5 Å resolution (Borowska et al., 2015). Crystallization leads from the other three DDM conditions are being optimized. Thus, *Mj*0480-specific sAB chaperones derived from nanodiscs enabled the production of diffraction-quality crystals of this small, archaeal membrane protein.

Similarly, despite multiple efforts, structure determination of the open, conductive conformation of CorA has been a challenging task (Pfoh et al., 2012). Here, the difficulties have been attributed to the high flexibility of CorA pentamer in the absence of magnesium ions (Dalmas et al., 2010, 2014; Pfoh et al., 2012), and strong crystal lattice effects, which cause CorA to collapse into a stable closed conformation (Eshaghi et al., 2006; Lunin et al., 2006; Payandeh and Pai, 2006). We investigated whether the open-state sABs could be used as potential crystallization chaperones of CorA in the absence of magnesium. For this, we obtained several stable sAB-CorA complexes only in the presence of EDTA, but not in Mg^{2+} conditions (e.g., sAB C10, C13, and C18 [Figure 5C]). Currently we test such sABs in high-throughput crystallization trials.

For *Mj*0480 and CorA, sABs obtained from library sorting experiments in nanodiscs show formation of stable and monodisperse complexes in size-exclusion chromatography. Such sABs can be used as robust crystallization chaperones and to facilitate the process of high-resolution structure determination. We believe this approach can be applied broadly to membrane proteins with different size and architecture.

DISCUSSION

Crystallization chaperones have enabled the determination of paradigm-shifting soluble and membrane protein structures (Koide, 2009; Bukowska and Grutter, 2013). There are several

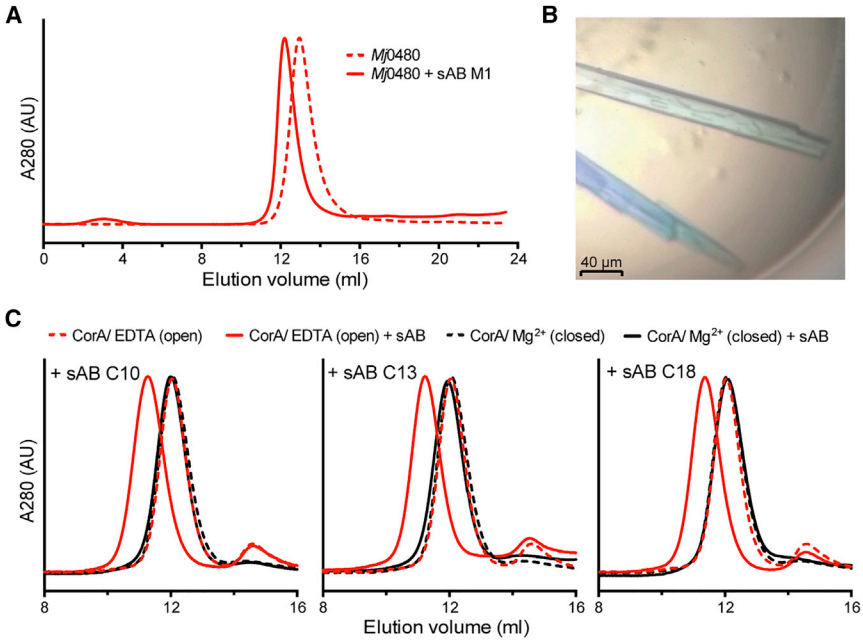

Figure 5. sABs Generated against Membrane Proteins in Nanodiscs as Crystallization Chaperones

(A) Size-exclusion chromatography shows specific shift of *Mj*0480 in the presence of sAB M1 (red, solid) in 0.05% DDM in comparison with *Mj*0480 run alone (red, dashed).

(B) Representative images of optimized *Mj*0480-sAB M1 crystals obtained in Peg/Ion Reagent 28 (Hampton).

(C) Size-exclusion chromatography showing a specific shift of CorA in the presence of sABs C10, C13, and C18 (red, solid) in 0.05% DDM and 1 mM EDTA in comparison with CorA alone (red, dashed). No complex formation is observed in the presence of Mg^{2+} (black; solid with sAB, dashed without sAB).

different types of crystallization chaperones and modes of generation, each with its own strengths and weaknesses (Koide, 2009; Bukowska and Grutter, 2013). Our work focuses on chaperones based on the Herceptin Fab framework. The size and compact shape of the Fab scaffold makes it ideal for most studies. It is about 440 amino acids and has been engineered for ultra-high stability (Eigenbrot et al., 1993). It displays efficiently on phage and expresses well in *E. coli*. The Fab chaperones are generated from fully synthetic phage display libraries in vitro, hence the name "synthetic antibodies" or sABs for short (Fellouse et al., 2004, 2007). Crystallization chaperones derived from library sorting methodologies are especially powerful because the biochemical conditions under which they are generated can be precisely controlled. Furthermore, the ability to select sABs that bind to different epitopes is a significant attribute. Besides their use as crystallization chaperones, sABs can be employed as customized fiducial markers for EM studies. In fact, this is more straightforward than making crystallization chaperones since essentially, all the sABs that bind tightly to the target proteins are potential candidates for EM applications.

We had previously been successful in generating high-performance sABs against detergent-solubilized membrane protein targets, but there were numerous difficulties with this approach often requiring extensive optimization on a case-by-case basis (Uysal et al., 2009; Li et al., 2014). We sought a more general and robust protocol of library sorting that minimizes the number of variables and time to complete the task, while maximizing the number of high-quality chaperones generated as the output. Ideally such a protocol would provide a more natural lipid environment and avoid the destabilizing effects of detergent. The implementation of nanodiscs into the selection pipeline has proved transformative in further exploiting the high-performance phage display selection capabilities.

Nanodisc-based library sorting experiments offer a number of key advantages. Nanodiscs are significantly more user-friendly than detergents because once embedded, the membrane proteins are easier to handle and more stable, and there is no need for the detergent optimization. In practice, selection experiments in nanodiscs are rapid (5 days), can be semi-automated, and, based on our experience with *Mj*0480, give rise to a larger pool of unique high-affinity sAB clones in comparison with standard selections in detergents. Importantly, phage display protocols in nanodiscs are modular. They can be tailored for applications where sABs for one or a few targets are desired, or can be easily expanded to accommodate medium- and high-throughput, fully automated pipelines. In addition, as shown by others, a large variety of membrane proteins of different origin, size, topology, stoichiometry, and organization can be readily incorporated into nanodiscs (Bayburt et al., 2006; Leitz et al., 2006; Borch and Hamann, 2009; Alvarez et al., 2010; Denisov and Sligar, 2011; Choi et al., 2013). Importantly, we find that as little as 200 μl of 2 μM antigen in biotinylated nanodiscs is sufficient for the successful library sorting even in cases where protein incorporation is problematic. This effectively expands the technology to many structurally challenging proteins and multi-component complexes.

It is generally appreciated that different detergents affect protein conformation and stability in different ways, and performing structure determination experiments in detergent environments raises issues about whether the resulting structures contain any detergent-induced artifacts (Barnett et al., 1996; Bamber et al., 2006; Cross et al., 2011). Thus, it is not surprising that our data show detergent-sensitive binding of the sABs to their protein target. Establishing exactly how dependent the protein properties are on detergent effects is difficult to determine experimentally. However, sABs generated using the nanodiscs provide a unique format for addressing this question. Strikingly, we found that the detergent "sensitivity" is epitope dependent—different sABs show different sensitivities in the same detergent. For example, the sAB M1-*Mj*0480 interaction is at least 1,000-fold tighter in nanodiscs and FC-12 than in DDM, whereas sAB

M4 binds *Mj*0480 equally well in both detergents and the nanodisc formats (Figure 3A).

There are two principal phenomena that may explain these observations. The first is a steric factor whereby differences in epitope availability can be dependent on the micelle size or chemical makeup of the detergent. The second relates to conformational factors, since there can be a difference in structure and local conformations of the epitope when the protein is in different environments (Laganowsky et al., 2014). In practice, some mixture of both mechanisms is probably important. Insight into the interplay of these factors is provided by the sAB M1-*Mj*0480 interaction, which displays significant sensitivity to DDM (but not FC-12). We showed that much of the binding to *Mj*0480 could be recovered in a lipid-dependent fashion by adding phospholipids to the protein before introducing it into the detergent (Figure 3C), suggesting that conformational effects, rather than steric factors, were predominant.

A question often raised is how tightly do the sABs have to bind their target to be effective crystallization chaperones? During crystallization the concentration of components generally is very high, such that binders even in the high-nanomolar range (~100–500 nM) could act as good chaperones. Nevertheless, there are arguments to be made for prioritizing toward choosing the highest-affinity candidates. Presumably, sABs that bind with high affinity (<10 nM) recognize low-energy conformational states, since if they bind to high energy non-native conformations there would be an energy cost to binding that would be reflected generally in a lower affinity. We see this with the conformation-specific sABs, which bind tightly in the conditions that stabilize the desired conformation, but lose affinity when the conditions change to favor an alternative conformation. sABs that retain their binding across multiple detergent types are also good candidates, since they recognize an epitope that is not highly influenced by the detergent.

In choosing a detergent, with all other things being equal, those that best reproduce the binding characteristics of a particular sAB in nanodiscs are obviously the best crystallization candidates, since the conformational state the sAB recognizes in a particular detergent is also found in the lipid environment. Conversely, loss of affinity going from the nanodisc to a detergent environment implies that the sAB had to expend energy to reorganize the binding epitope. However, our finding that adding small amounts of lipid to the protein-detergent mix may rescue sAB binding affinities suggests that this may be a useful step that should be tried before triaging a sAB from the pool of candidate chaperones. This is likewise important for EM studies whereby affinity is more important than for crystallization chaperones since the concentrations are considerably lower. In addition, the technology to collect EM data on nanodisc-embedded targets is being further developed and offers the opportunity to quickly provide microscopists ready-made systems with customized fiducial markers (Frauenfeld et al., 2011; Wu et al., 2012; Choi et al., 2013; Gogol et al., 2013).

EXPERIMENTAL PROCEDURES

Protein Production and Biotinylation

Plasmid harboring the N-terminal hexahistidine construct of membrane scaffold protein (MSP1) E3D1 (pMSP1E3D1) of the nanodiscs was obtained from Addgene (#20066). His-MSP1 E3D1 was expressed, purified, and cleaved with tobacco etch virus protease according to protocols described previously (Alvarez et al., 2010). Cleaved MSP1 E3D1 was desalted on PD-10 columns (GE Healthcare) against buffer A (50 mM HEPES [pH 7.5] and 200 mM NaCl). For preparations of biotinylated nanodiscs, MSP1 E3D1 was biotinylated using 5-fold molar excess of biotinylation reagent EZ-Link-NHS-PEG4-Biotin (Thermo) for 1 hr at room temperature. The reaction was quenched with 5 mM final concentration of Tris (pH 7.5), and the excess NHS reagent was removed with PD-10 columns.

N-Terminal hexahistidine constructs of *Mj*0480 and two variants of *T. maritima* CorA (wild-type and D253K) were expressed and purified as previously described (Dalmas et al., 2010; Borowska et al., 2015). Biotinylated versions of *Mj*0480 and CorA wild-type in detergent were prepared using 20- and 5-fold molar excess of EZ-Link-NHS-SS-PEG4-Biotin (Thermo), respectively in buffer containing 10 mM HEPES (pH 7.5), 200 mM NaCl, and either 0.05% n-dodecyl-β-D-maltoside (DDM, Affymetrix) or 0.1% Fos-Choline-12 (FC-12, Affymetrix) for *Mj*0480, and 25 mM HEPES (pH 7.5), 150 mM NaCl, 0.05% DDM, and 20 mM $MgCl_2$ for CorA wild-type. Excess NHS reagent was removed by size-exclusion chromatography on a Superdex200 10/300 GL column.

Synthetic antibody fragments (sABs) in pSFV4 or pRH2.2 vectors (kindly provided by SGC Toronto and S. Sidhu, respectively) were expressed and purified as described previously (Borowska et al., 2015) in a two-step purification protocol on MabSelect SuRe Protein A column (GE Healthcare) and cation exchange Resource S 1 ml column (GE Healthcare), and were dialyzed into buffer A.

Non-biotinylated and biotinylated versions of MSP1 E3D1 and membrane proteins as well as purified sABs were concentrated, aliquoted, flash-frozen in liquid nitrogen, and kept at −80°C.

Nanodisc Reconstitution

Reconstitution of *Mj*0480 and two variants of CorA (wild-type and D253K) into E3D1 nanodiscs was performed according to the protocols described by the Sligar laboratory (Ritchie et al., 2009) with two modifications: (1) biotinylated cleaved MSP1 E3D1 was used to generate biotinylated nanodiscs; (2) lipids used for reconstitution were solubilized using either DDM, or n-undecyl-β-D-maltoside (UDM, Affymetrix) in place of sodium cholate. His-tagged membrane proteins were reconstituted into nanodiscs using either biotinylated or non-biotinylated MSP1 E3D1 and various phospholipid compositions to generate following E3D1 nanodiscs: *Mj*0480 in eggPC, *Mj*0480 in 1,2-dimyristoyl-*sn*-glycero-3-phosphocholine (DMPC), CorA wild-type in palmitoyloleoylphosphatidylcholine/palmitoyloleoylphosphatidylglycerol (POPC/POPG), and CorA D253K in POPC/POPG nanodiscs. Nanodiscs with membrane proteins embedded were separated from empty nanodiscs by metal affinity chromatography in batch using Ni-NTA Superflow resin (Qiagen) and further purified on a Superdex200 10/300 GL column in buffer A. As a control, empty E3D1 nanodiscs were prepared using the same phospholipids. All nanodisc samples were concentrated, supplemented with 5% (w/v) sucrose, aliquoted, flash-frozen in liquid nitrogen, and kept at −80°C. Detailed procedures of preparation of phospholipids and nanodisc reconstitution are described in the Supplemental Experimental Procedures.

Phage Library Sorting

To generate sABs, we performed five independent library sorting experiments against the following biotinylated antigens: (1) *Mj*0480 in eggPC nanodiscs, (2) *Mj*0480 in DMPC nanodiscs, (3) *Mj*0480 in DDM, (4) CorA wild-type in POPC/POPG nanodiscs, and (5) as in (4) with CorA D253K in non-biotinylated POPC/POPG nanodiscs as soluble competitor. Prior to library sorting, the efficiency of biotinylation of antigens was evaluated by pull-down on streptavidin-coated magnetic beads (Streptavidin MagneSpehere Paramagnetic particles, Promega). Library sorting steps were performed using sAB Library E (kindly provided by S. Koide [Miller et al., 2012]) based on described protocols (Fellouse et al., 2007; Koide et al., 2009; Paduch et al., 2013; Dominik and Kossiakoff, 2015) with the following modifications: (1) five, instead of four, rounds of library sorting were performed; (2) experiments with nanodiscs were performed in either buffer B (1% BSA in buffer A) or buffer C (1 mM EDTA in buffer B for CorA wild-type), while experiments with *Mj*0480 in detergent were performed in buffer D (buffer B with 0.05% DDM); (3) for experiments with nanodiscs, starting from the second sorting round, non-biotinylated empty nanodiscs

(and, where indicated, CorA D253K nanodiscs) were used as soluble competitors; (4) elution of phage particles in experiments with nanodiscs and detergent were achieved by incubation in buffer B supplemented with 1% FC-12 and 100 mM DDT, respectively. The details of the strategy along with concentrations of membrane protein antigens throughout the library sorting experiments are further described in Supplemental Experimental Procedures.

Phage and Protein ELISA Assays

Single-point phage ELISA was used in the primary validation of binding affinities of generated sABs in phage format as described previously (Dominik and Kossiakoff, 2015). Amplified phage particles at 10-fold dilution were assayed against 20 nM biotinylated membrane proteins in either nanodiscs or detergent using HRP-conjugated anti-M13 monoclonal antibody (GE Healthcare, #27-9421-01). Assays were performed in library sorting buffer (buffer A–D depending on the target, as described above) supplemented with 2% BSA instead of 1%. Each sAB clone with A_{450} signal above 0.2 (four times the average background level of the assay) was sequenced; unique sABs were sub-cloned into pSVF4 or pRH2.2 vectors, and purified as described above.

Multi-point protein ELISA was used to estimate the apparent binding affinity (EC_{50} values) of purified sABs. Purified sABs in 3-fold serial dilution starting from 5 μM were assayed against membrane proteins either biotinylated in detergents or in biotinylated nanodiscs at 20 nM, as indicated. The binding signal (A_{450}) was detected using HRP-conjugated anti-human $(Fab)_2$ antibody (Peroxidase-conjugated AffiniPure Goat, Jackson ImmunoResearch #109-035-006). A_{450} values were normalized for the minimum and maximum signal intensity in each series, plotted against log of sAB concentration, and EC_{50} values were calculated assuming sigmoidal dose response with a variable slope model using GraphPad Prism (GraphPad Software). Data points from three independent experiments in triplicates represent mean values with error bars denoting SD value from the mean.

To determine the influence of phospholipids on binding of sABs M1 and M4 to *Mj*0480 in 0.05% DDM, we performed single-point protein ELISA essentially as in the procedure described above, except that 1 mM eggPC in 0.15% DDM in buffer A was added onto immobilized biotinylated *Mj*0480, followed by 30 min incubation, and washing with buffer A. Constant concentration of sAB M1 and M4 below the established EC_{50} values for the *Mj*0480 in DDM (100 and 1 nM, respectively) was used for binding. Data points from three independent experiments in triplicates represent mean values with error bars denoting SD value from the mean.

Complex Formation and Crystallization Trials

To form the protein-sAB complexes we incubated *Mj*0480 with a saturating amount of sAB M1, and complex was purified and crystallized as previously described (Borowska et al., 2015). Complexes of CorA wild-type with sABs C10, C13, and C18 at 1:1.2 fold molar ratio were injected onto a Superdex200 10/300 GL column equilibrated with buffer containing 20 mM HEPES (pH 7.5), 150 mM NaCl, 0.025% DDM, and either 1 mM EDTA or 20 mM $MgCl_2$. In all cases, a membrane protein only control was included. Peak fractions corresponding to the CorA-sAB complexes in 1 mM EDTA were concentrated to 7–10 mg/ml. Subsequently, high-throughput crystallization screens were set up using Mosquito robot (TPP Labtech) at 100 nl of protein and 100 nl of reservoir solution, and crystals were grown by the hanging-drop vapor diffusion method.

SUPPLEMENTAL INFORMATION

Supplemental Information includes Supplemental Experimental Procedures, five figures, and one table and can be found with this article online at http://dx.doi.org/10.1016/j.str.2015.11.014.

AUTHOR CONTRIBUTIONS

P.K.D. performed nanodisc reconstitution, sAB selections, and initial validation of sAB clones. M.T.B., O.D., and P.K.D. carried out the expression and purification of proteins, designed library sorting strategies, and optimized binding experiments. S.S.K. carried out the binding experiments. A.A.K. and P.K.D. designed experiments, with assistance from R.J.K. and E.P. P.K.D. and A.A.K. wrote the manuscript with input from all authors.

ACKNOWLEDGMENTS

We thank S. Koide for providing the DNA of phage Library E; B.E. Zalisko for advice on nanodiscs reconstitution; M.L. Paduch and A. Koide for discussion on library sorting strategies with nanodiscs; B.G. Fox and members of his laboratory for sharing the data on optimization of nanodisc elution from a solid surface; K. Sheehy and L.J. Bailey for help with manuscript preparation; and other members of the Kossiakoff, Keenan, and Perozo labs (especially M. Nocula-Lugowska and S. Mukherjee) for support and useful comments on experiments. This work was supported by NIH grants U01 GM094588 (to A.A.K.), U54 GM087519 (to A.A.K. and E.P.), GM088406 (to E.P.), and R01 GM086487 (to R.J.K.). We also acknowledge support from the Searle Funds at the Chicago Community Trust for the Chicago Biomedical Consortium (to A.A.K. and R.J.K.).

Received: August 18, 2015
Revised: November 20, 2015
Accepted: November 23, 2015
Published: December 31, 2015

REFERENCES

Alvarez, F.J., Orelle, C., and Davidson, A.L. (2010). Functional reconstitution of an ABC transporter in nanodiscs for use in electron paramagnetic resonance spectroscopy. J. Am. Chem. Soc. *132*, 9513–9515.

Bamber, L., Harding, M., Butler, P.J., and Kunji, E.R. (2006). Yeast mitochondrial ADP/ATP carriers are monomeric in detergents. Proc. Natl. Acad. Sci. USA *103*, 16224–16229.

Barnett, S.M., Dracheva, S., Hendler, R., and Levin, I.W. (1996). Lipid-induced conformational changes of an integral membrane protein: an infrared spectroscopic study of the effects of Triton X-100 treatment on the purple membrane of *Halobacterium halobium* ET1001. Biochemistry *35*, 4558–4567.

Bayburt, T.H., and Sligar, S.G. (2010). Membrane protein assembly into nanodiscs. FEBS Lett. *584*, 1721–1727.

Bayburt, T.H., Grinkova, Y.V., and Sligar, S.G. (2006). Assembly of single bacteriorhodopsin trimers in bilayer nanodiscs. Arch. Biochem. Biophys. *450*, 215–222.

Borch, J., and Hamann, T. (2009). The nanodisc: a novel tool for membrane protein studies. Biol. Chem. *390*, 805–814.

Borowska, M.T., Dominik, P.K., Anghel, S.A., Kossiakoff, A.A., and Keenan, R.J. (2015). A YidC-like protein in the archaeal plasma membrane. Structure *23*, 1715–1724.

Bukowska, M.A., and Grutter, M.G. (2013). New concepts and aids to facilitate crystallization. Curr. Opin. Struct. Biol. *23*, 409–416.

Choi, W.S., Rice, W.J., Stokes, D.L., and Coller, B.S. (2013). Three-dimensional reconstruction of intact human integrin alphaIIbbeta3: new implications for activation-dependent ligand binding. Blood *122*, 4165–4171.

Chung, K.Y., Kim, T.H., Manglik, A., Alvares, R., Kobilka, B.K., and Prosser, R.S. (2012). Role of detergents in conformational exchange of a G protein-coupled receptor. J. Biol. Chem. *287*, 36305–36311.

Cross, T.A., Sharma, M., Yi, M., and Zhou, H.X. (2011). Influence of solubilizing environments on membrane protein structures. Trends Biochem. Sci. *36*, 117–125.

Dalmas, O., Cuello, L.G., Jogini, V., Cortes, D.M., Roux, B., and Perozo, E. (2010). Structural dynamics of the magnesium-bound conformation of CorA in a lipid bilayer. Structure *18*, 868–878.

Dalmas, O., Sompornpisut, P., Bezanilla, F., and Perozo, E. (2014). Molecular mechanism of Mg^{2+}-dependent gating in CorA. Nat. Commun. *5*, 3590.

Denisov, I.G., and Sligar, S.G. (2011). Cytochromes P450 in nanodiscs. Biochim. Biophys. Acta *1814*, 223–229.

Dominik, P.K., and Kossiakoff, A.A. (2015). Phage display selections for affinity reagents to membrane proteins in nanodiscs. Methods Enzymol. *557*, 219–245.

Eigenbrot, C., Randal, M., Presta, L., Carter, P., and Kossiakoff, A.A. (1993). X-ray structures of the antigen-binding domains from three variants of

humanized anti-p185HER2 antibody 4D5 and comparison with molecular modeling. J. Mol. Biol. *229*, 969–995.

Eshaghi, S., Niegowski, D., Kohl, A., Martinez Molina, D., Lesley, S.A., and Nordlund, P. (2006). Crystal structure of a divalent metal ion transporter CorA at 2.9 angstrom resolution. Science *313*, 354–357.

Fellouse, F.A., Wiesmann, C., and Sidhu, S.S. (2004). Synthetic antibodies from a four-amino-acid code: a dominant role for tyrosine in antigen recognition. Proc. Natl. Acad. Sci. USA *101*, 12467–12472.

Fellouse, F.A., Esaki, K., Birtalan, S., Raptis, D., Cancasci, V.J., Koide, A., Jhurani, P., Vasser, M., Wiesmann, C., Kossiakoff, A.A., et al. (2007). High-throughput generation of synthetic antibodies from highly functional minimalist phage-displayed libraries. J. Mol. Biol. *373*, 924–940.

Frauenfeld, J., Gumbart, J., Sluis, E.O., Funes, S., Gartmann, M., Beatrix, B., Mielke, T., Berninghausen, O., Becker, T., Schulten, K., et al. (2011). Cryo-EM structure of the ribosome-SecYE complex in the membrane environment. Nat. Struct. Mol. Biol. *18*, 614–621.

Gogol, E.P., Akkaladevi, N., Szerszen, L., Mukherjee, S., Chollet-Hinton, L., Katayama, H., Pentelute, B.L., Collier, R.J., and Fisher, M.T. (2013). Three dimensional structure of the anthrax toxin translocon-lethal factor complex by cryo-electron microscopy. Protein Sci. *22*, 586–594.

Hagn, F., Etzkorn, M., Raschle, T., and Wagner, G. (2013). Optimized phospholipid bilayer nanodiscs facilitate high-resolution structure determination of membrane proteins. J. Am. Chem. Soc. *135*, 1919–1925.

Kim, J., Stroud, R.M., and Craik, C.S. (2011). Rapid identification of recombinant Fabs that bind to membrane proteins. Methods *55*, 303–309.

Koide, S. (2009). Engineering of recombinant crystallization chaperones. Curr. Opin. Struct. Biol. *19*, 449–457.

Koide, A., Wojcik, J., Gilbreth, R.N., Reichel, A., Piehler, J., and Koide, S. (2009). Accelerating phage-display library selection by reversible and site-specific biotinylation. Protein Eng. Des. Sel. *22*, 685–690.

Laganowsky, A., Reading, E., Allison, T.M., Ulmschneider, M.B., Degiacomi, M.T., Baldwin, A.J., and Robinson, C.V. (2014). Membrane proteins bind lipids selectively to modulate their structure and function. Nature *510*, 172–175.

Leitz, A.J., Bayburt, T.H., Barnakov, A.N., Springer, B.A., and Sligar, S.G. (2006). Functional reconstitution of Beta2-adrenergic receptors utilizing self-assembling nanodisc technology. Biotechniques *40*, 601–602, 604, 606, passim.

Li, Q., Wanderling, S., Paduch, M., Medovoy, D., Singharoy, A., McGreevy, R., Villalba-Galea, C.A., Hulse, R.E., Roux, B., Schulten, K., et al. (2014). Structural mechanism of voltage-dependent gating in an isolated voltage-sensing domain. Nat. Struct. Mol. Biol. *21*, 244–252.

Lunin, V.V., Dobrovetsky, E., Khutoreskaya, G., Zhang, R., Joachimiak, A., Doyle, D.A., Bochkarev, A., Maguire, M.E., Edwards, A.M., and Koth, C.M. (2006). Crystal structure of the CorA Mg^{2+} transporter. Nature *440*, 833–837.

Mateja, A., Paduch, M., Chang, H.Y., Szydlowska, A., Kossiakoff, A.A., Hegde, R.S., and Keenan, R.J. (2015). Protein targeting. Structure of the Get3 targeting factor in complex with its membrane protein cargo. Science *347*, 1152–1155.

Miller, K.R., Koide, A., Leung, B., Fitzsimmons, J., Yoder, B., Yuan, H., Jay, M., Sidhu, S.S., Koide, S., and Collins, E.J. (2012). T cell receptor-like recognition of tumor in vivo by synthetic antibody fragment. PLoS One *7*, e43746.

Moomaw, A.S., and Maguire, M.E. (2008). The unique nature of Mg^{2+} channels. Physiology (Bethesda) *23*, 275–285.

Niegowski, D., and Eshaghi, S. (2007). The CorA family: structure and function revisited. Cell Mol. Life Sci. *64*, 2564–2574.

Paduch, M., Koide, A., Uysal, S., Rizk, S.S., Koide, S., and Kossiakoff, A.A. (2013). Generating conformation-specific synthetic antibodies to trap proteins in selected functional states. Methods *60*, 3–14.

Payandeh, J., and Pai, E.F. (2006). A structural basis for Mg^{2+} homeostasis and the CorA translocation cycle. EMBO J. *25*, 3762–3773.

Payandeh, J., Li, C., Ramjeesingh, M., Poduch, E., Bear, C.E., and Pai, E.F. (2008). Probing structure-function relationships and gating mechanisms in the CorA Mg^{2+} transport system. J. Biol. Chem. *283*, 11721–11733.

Pfoh, R., Li, A., Chakrabarti, N., Payandeh, J., Pomes, R., and Pai, E.F. (2012). Structural asymmetry in the magnesium channel CorA points to sequential allosteric regulation. Proc. Natl. Acad. Sci. USA *109*, 18809–18814.

Ritchie, T.K., Grinkova, Y.V., Bayburt, T.H., Denisov, I.G., Zolnerciks, J.K., Atkins, W.M., and Sligar, S.G. (2009). Chapter 11—Reconstitution of membrane proteins in phospholipid bilayer nanodiscs. Methods Enzymol. *464*, 211–231.

Rizk, S.S., Paduch, M., Heithaus, J.H., Duguid, E.M., Sandstrom, A., and Kossiakoff, A.A. (2011). Allosteric control of ligand-binding affinity using engineered conformation-specific effector proteins. Nat. Struct. Mol. Biol. *18*, 437–442.

Sonoda, Y., Newstead, S., Hu, N.J., Alguel, Y., Nji, E., Beis, K., Yashiro, S., Lee, C., Leung, J., Cameron, A.D., et al. (2011). Benchmarking membrane protein detergent stability for improving throughput of high-resolution X-ray structures. Structure *19*, 17–25.

Uysal, S., Vasquez, V., Tereshko, V., Esaki, K., Fellouse, F.A., Sidhu, S.S., Koide, S., Perozo, E., and Kossiakoff, A. (2009). Crystal structure of full-length KcsA in its closed conformation. Proc. Natl. Acad. Sci. USA *106*, 6644–6649.

Wu, S., Avila-Sakar, A., Kim, J., Booth, D.S., Greenberg, C.H., Rossi, A., Liao, M., Li, X., Alian, A., Griner, S.L., et al. (2012). Fabs enable single particle cryoEM studies of small proteins. Structure *20*, 582–592.

Structure, Volume *24*

Supplemental Information

Conformational Chaperones for Structural Studies of Membrane Proteins Using Antibody Phage Display with Nanodiscs

Pawel K. Dominik, Marta T. Borowska, Olivier Dalmas, Sangwoo S. Kim, Eduardo Perozo, Robert J. Keenan, and Anthony A. Kossiakoff

SUPPLEMENTAL FIGURES AND LEGENDS

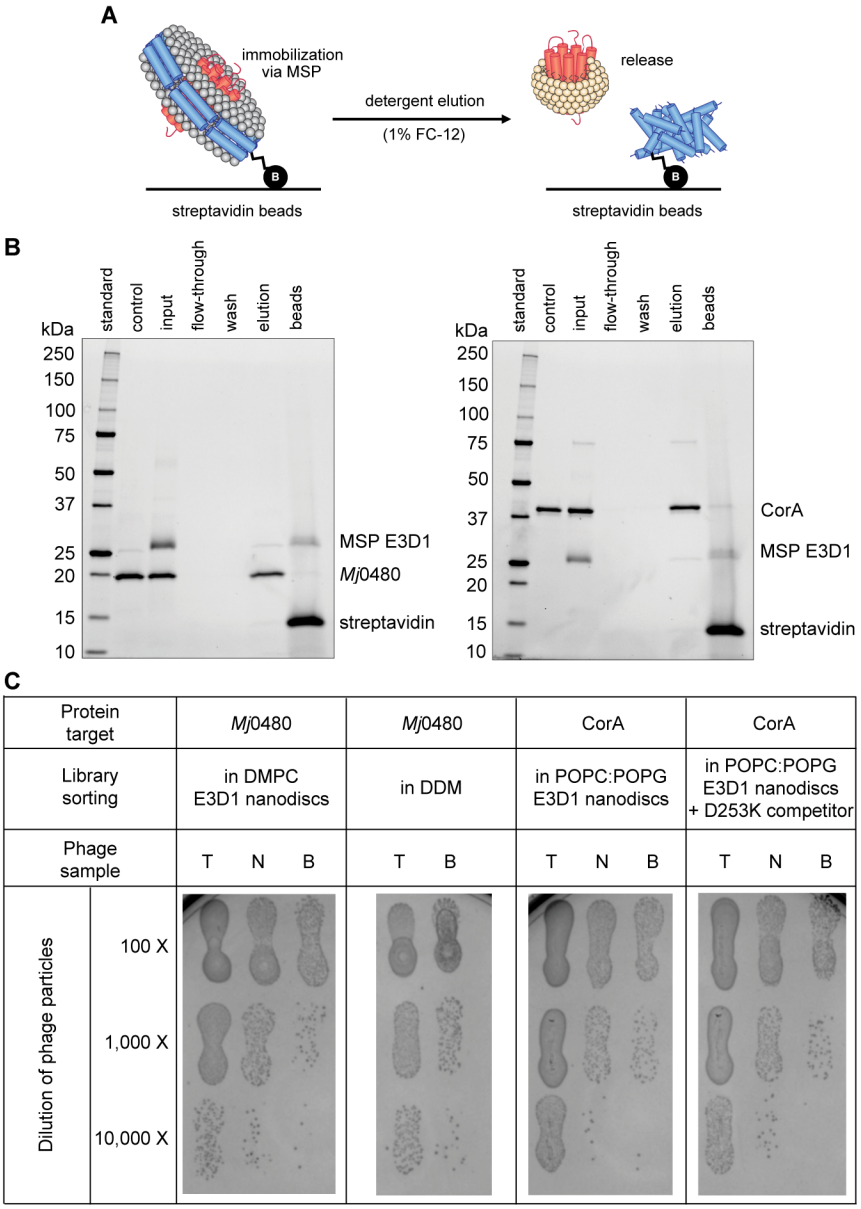

Figure S1. Incorporation of nanodiscs into library sorting pipeline. (Related to Figure 1) (A) Reversible immobilization of *Mj*0480 and CorA in biotinylated nanodiscs. *M. jannaschii* *Mj*0480 and *T. maritima* CorA were reconstituted into E3D1 nanodiscs. Biotinylated nanodiscs with target protein were incubated with streptavidin-coated magnetic beads and washed to remove excess of unbound sample. To disassemble nanodiscs and release *Mj*0480 and CorA into solution, beads were incubated in 1% fos-choline-12 (FC-12, yellow spheres). The biotinylated membrane scaffold protein E3D1 (MSP E3D1; blue) remained on the surface of the beads. (B)

SDS-PAGE analysis of the pull-down experiment described in (A) shows efficient immobilization of both *Mj*0480 (left) and CorA (right) in biotinylated E3D1 nanodiscs onto solid surface, and a robust elution of both proteins from the streptavidin beads. Equal volumes of input, flow-through, first wash, elution and beads fractions, along with protein only controls are shown on the gel. (C) Enrichment of eluted phage particles after fifth round of phage display library sorting against *Mj*0480 and CorA. Phage particles eluted with FC-12 (or DTT, for library sorting with DDM) after fifth sorting round were used for infection of *E. coli* XL-1 strain (Stratagene) and plated in serial dilutions on LB agar plates supplemented with ampicillin. The amount of eluted phage particles was compared between experiments performed in the presence of: T – target membrane protein (either in nanodiscs or in DDM, as indicated), N – empty nanodiscs, B – empty streptavidin-coated magnetic beads. No enrichment analysis for empty nanodiscs was performed for experiment with *Mj*0480 in DDM as empty nanodiscs were not present throughout library sorting.

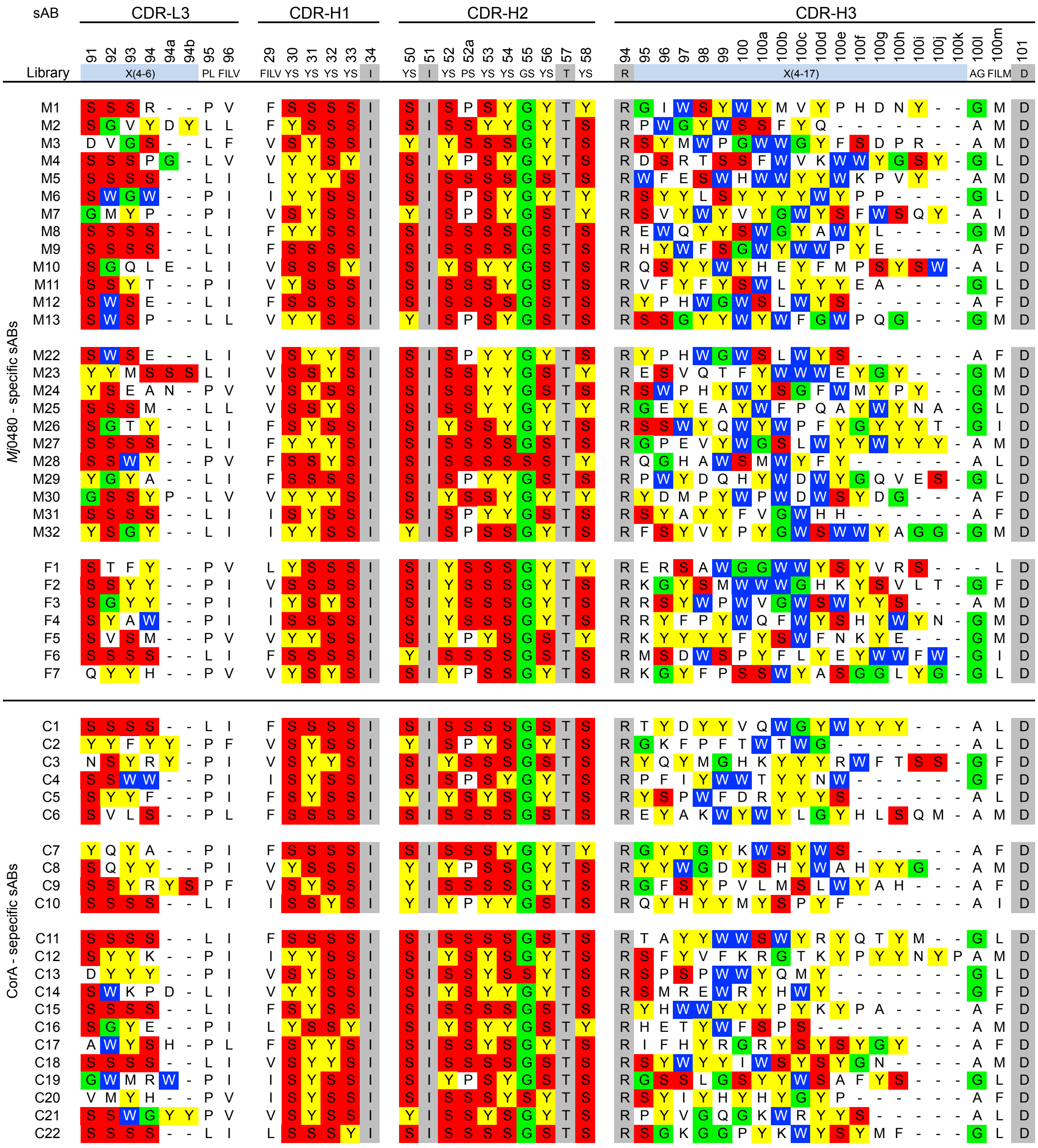

	sAB	CDR-L3								CDR-H1						CDR-H2										CDR-H3																				
		91	92	93	94	94a	94b	95	96	29	30	31	32	33	34	50	51	52	52a	53	54	55	56	57	58	94	95	96	97	98	99	100	100a	100b	100c	100d	100e	100f	100g	100h	100i	100j	100k	100l	100m	101
	Library	X(4-6)						PL	FILV	FILV	YS	YS	YS	YS	I	YS	I	YS	PS	YS	YS	GS	YS	T	YS	R	X(4-17)																	AG	FILM	D
*Mj*0480 - specific sABs	M1	S	S	S	R	-	-	P	V	F	S	S	S	S	I	S	I	S	P	S	Y	G	Y	T	Y	R	G	I	W	S	Y	W	Y	M	V	Y	P	H	D	N	Y	-	-	G	M	D
	M2	S	G	V	Y	D	Y	L	L	F	Y	S	S	S	I	S	I	S	S	Y	Y	G	Y	T	S	R	P	W	G	Y	W	S	S	F	Y	Q	-	-	-	-	-	-	-	A	M	D
	M3	D	V	G	S	-	-	L	F	V	S	Y	S	S	I	Y	I	Y	S	S	S	G	Y	T	S	R	S	Y	M	W	P	G	W	W	G	Y	F	S	D	P	R	-	-	A	M	D
	M4	S	S	S	P	G	-	L	V	V	Y	Y	S	Y	I	S	I	Y	P	S	Y	G	Y	T	S	R	D	S	R	T	S	S	F	W	V	K	W	W	Y	G	S	Y	-	G	L	D
	M5	S	S	S	S	-	-	L	I	L	Y	Y	Y	S	I	S	I	S	S	S	S	G	S	T	S	R	W	F	E	S	W	H	W	W	Y	Y	W	K	P	V	Y	-	-	A	M	D
	M6	S	W	G	W	-	-	P	I	I	Y	Y	S	S	I	S	I	S	P	S	Y	G	Y	T	Y	R	S	Y	Y	L	S	Y	Y	Y	Y	W	Y	P	P	-	-	-	-	G	L	D
	M7	G	M	Y	P	-	-	P	I	V	S	Y	S	S	I	Y	I	S	P	S	Y	G	S	T	Y	R	S	V	Y	W	Y	V	Y	G	W	Y	S	F	W	S	Q	Y	-	A	I	D
	M8	S	S	S	S	-	-	L	I	F	Y	Y	S	S	I	S	I	S	S	S	S	G	S	T	S	R	E	W	Q	Y	Y	S	W	G	Y	A	W	Y	L	-	-	-	-	G	M	D
	M9	S	S	S	S	-	-	L	I	F	S	S	S	S	I	S	I	S	S	S	S	G	S	T	S	R	H	Y	W	F	S	G	W	Y	W	W	P	Y	E	-	-	-	-	A	F	D
	M10	S	G	Q	L	E	-	L	I	V	S	S	S	Y	I	S	I	Y	S	Y	Y	G	S	T	S	R	Q	S	Y	Y	W	Y	H	E	Y	F	M	P	S	Y	S	W	-	A	L	D
	M11	S	S	Y	T	-	-	P	I	V	Y	S	S	S	I	S	I	S	S	S	Y	G	S	T	S	R	V	F	Y	F	Y	S	W	L	Y	Y	Y	E	A	-	-	-	-	G	L	D
	M12	S	W	S	E	-	-	L	I	F	S	S	S	S	I	S	I	S	S	S	S	G	S	T	S	R	Y	P	H	W	G	W	S	L	W	Y	S	-	-	-	-	-	-	A	F	D
	M13	S	W	S	P	-	-	L	L	V	Y	Y	S	S	I	Y	I	S	P	S	Y	G	S	T	S	R	S	S	G	Y	Y	W	Y	W	F	G	W	P	Q	G	-	-	-	G	M	D
	M22	S	W	S	E	-	-	L	I	V	S	Y	Y	S	I	S	I	S	P	Y	Y	G	Y	T	S	R	Y	P	H	W	G	W	S	L	W	Y	S	-	-	-	-	-	-	A	F	D
	M23	Y	Y	M	S	S	S	L	I	V	S	S	Y	S	I	S	I	S	S	Y	Y	G	S	T	Y	R	E	S	V	Q	T	F	Y	W	W	W	E	Y	G	Y	-	-	-	G	M	D
	M24	Y	S	E	A	N	-	P	V	V	S	Y	S	S	I	S	I	S	S	Y	Y	G	S	T	S	R	S	W	P	H	Y	W	Y	S	G	F	W	M	Y	P	Y	-	-	G	M	D
	M25	S	S	S	M	-	-	L	L	V	S	S	Y	S	I	S	I	S	S	Y	Y	G	Y	T	Y	R	G	E	Y	E	A	Y	W	F	P	Q	A	Y	W	Y	N	A	-	G	L	D
	M26	S	G	T	Y	-	-	L	I	F	S	Y	S	S	I	S	I	Y	S	S	Y	G	Y	T	S	R	S	S	W	Y	Q	W	Y	W	P	F	Y	G	Y	Y	Y	T	-	G	I	D
	M27	S	S	S	S	-	-	L	I	F	Y	Y	Y	S	I	S	I	S	S	S	S	G	S	T	S	R	G	P	E	V	Y	W	G	S	L	W	Y	Y	W	Y	Y	Y	-	A	M	D
	M28	S	S	W	Y	-	-	P	V	F	S	S	Y	S	I	S	I	S	S	S	S	S	S	T	Y	R	Q	G	H	A	W	S	M	W	Y	F	Y	-	-	-	-	-	-	A	L	D
	M29	Y	G	Y	A	-	-	L	I	F	S	S	S	S	I	S	I	S	P	Y	Y	G	S	T	S	R	P	W	Y	D	Q	H	Y	W	D	W	Y	G	Q	V	E	S	-	G	L	D
	M30	G	S	S	Y	P	-	L	V	V	Y	Y	Y	S	I	S	I	Y	S	S	Y	G	Y	T	Y	R	Y	D	M	P	Y	W	P	W	D	W	S	Y	D	G	-	-	-	A	F	D
	M31	S	S	S	S	-	-	L	I	I	S	Y	S	S	I	S	I	S	P	Y	Y	G	S	T	S	R	S	Y	A	Y	Y	F	V	G	W	H	H	-	-	-	-	-	-	A	F	D
	M32	Y	S	G	Y	-	-	L	I	I	Y	Y	S	S	I	Y	I	S	P	S	S	G	Y	T	S	R	F	S	Y	V	Y	P	Y	G	W	S	W	W	Y	A	G	G	-	G	M	D
	F1	S	T	F	Y	-	-	P	V	L	Y	S	S	S	I	S	I	Y	S	S	S	G	Y	T	Y	R	E	R	S	A	W	G	G	W	W	Y	S	Y	V	R	S	-	-	-	L	D
	F2	S	S	Y	Y	-	-	P	I	V	S	S	S	S	I	S	I	Y	S	S	S	G	Y	T	S	R	K	G	Y	S	M	W	W	W	G	H	K	Y	S	V	L	T	-	G	F	D
	F3	S	G	Y	Y	-	-	P	I	I	Y	S	Y	S	I	S	I	Y	S	S	S	G	Y	T	S	R	R	S	Y	W	P	W	V	G	W	S	W	Y	Y	S	-	-	-	A	M	D
	F4	S	Y	A	W	-	-	P	I	I	S	S	S	S	I	S	I	Y	S	S	S	G	Y	T	S	R	R	Y	F	P	Y	W	Q	F	W	Y	S	H	Y	W	Y	N	-	G	M	D
	F5	S	V	S	M	-	-	P	V	V	Y	Y	S	S	I	S	I	Y	P	Y	S	G	S	T	Y	R	K	Y	Y	Y	Y	F	Y	S	W	F	N	K	Y	E	-	-	-	G	M	D
	F6	S	S	S	S	-	-	L	I	F	S	S	S	S	I	Y	I	S	S	S	S	G	S	T	S	R	M	S	D	W	S	P	Y	F	L	Y	E	Y	W	W	F	W	-	G	I	D
	F7	Q	Y	Y	H	-	-	P	V	V	Y	S	Y	S	I	S	I	Y	P	S	S	G	Y	T	S	R	K	G	Y	F	P	S	S	W	Y	A	S	G	G	L	Y	G	-	G	L	D
CorA - sepecific sABs	C1	S	S	S	S	-	-	L	I	F	S	S	S	S	I	S	I	S	S	S	S	G	S	T	S	R	T	Y	D	Y	Y	V	Q	W	G	Y	W	Y	Y	Y	-	-	-	A	L	D
	C2	Y	Y	F	Y	Y	-	P	F	V	S	Y	S	S	I	Y	I	S	P	Y	S	G	Y	T	S	R	G	K	F	P	F	T	W	T	W	G	-	-	-	-	-	-	-	A	L	D
	C3	N	S	Y	R	Y	-	P	I	V	S	Y	Y	S	I	S	I	Y	S	S	S	G	S	T	S	R	Y	Q	Y	M	G	H	K	Y	Y	Y	R	W	F	T	S	S	-	G	F	D
	C4	S	S	W	W	-	-	P	I	I	S	Y	S	S	I	S	I	S	P	S	Y	G	Y	T	S	R	P	F	I	Y	W	W	T	Y	Y	N	W	-	-	-	-	-	-	G	F	D
	C5	S	Y	Y	F	-	-	P	I	F	S	Y	S	S	I	Y	I	Y	S	Y	S	G	Y	T	S	R	Y	S	P	W	F	D	R	Y	Y	Y	S	-	-	-	-	-	-	A	L	D
	C6	S	V	L	S	-	-	P	L	F	S	S	S	S	I	S	I	S	S	S	S	G	S	T	S	R	E	Y	A	K	W	Y	W	Y	L	G	Y	H	L	S	Q	M	-	A	M	D
	C7	Y	Q	Y	A	-	-	P	I	F	S	S	S	S	I	S	I	S	S	S	Y	G	Y	T	Y	R	G	Y	Y	G	Y	K	W	S	Y	W	S	-	-	-	-	-	-	A	F	D
	C8	S	Q	Y	Y	-	-	P	I	V	Y	S	S	S	I	Y	I	Y	P	S	S	G	Y	T	S	R	Y	Y	W	G	D	Y	S	H	Y	W	A	H	Y	Y	G	-	-	A	M	D
	C9	S	S	Y	R	Y	S	P	F	V	S	Y	S	S	I	Y	I	S	S	S	S	G	Y	T	S	R	G	F	S	Y	P	V	L	M	S	L	W	Y	A	H	-	-	-	A	F	D
	C10	S	S	S	S	-	-	L	I	I	S	S	Y	S	I	Y	I	Y	P	Y	Y	G	S	T	S	R	Q	Y	H	Y	Y	M	Y	S	P	Y	F	-	-	-	-	-	-	A	I	D
	C11	S	S	S	S	-	-	L	I	F	S	S	S	S	I	S	I	S	S	S	S	G	S	T	S	R	T	A	Y	Y	W	W	S	W	Y	R	Y	Q	T	Y	M	-	-	G	L	D
	C12	S	Y	Y	K	-	-	P	I	I	Y	Y	S	S	I	S	I	Y	S	Y	S	G	Y	T	S	R	S	F	Y	V	F	K	R	G	T	K	Y	P	Y	Y	N	Y	P	A	M	D
	C13	D	Y	Y	Y	-	-	P	I	V	S	Y	S	S	I	S	I	S	S	Y	S	S	Y	T	S	R	S	P	S	P	W	W	Y	Q	M	Y	-	-	-	-	-	-	-	G	L	D
	C14	S	W	K	P	D	-	L	I	V	Y	Y	S	S	I	S	I	Y	S	Y	Y	G	Y	T	S	R	S	M	R	E	W	R	Y	H	W	Y	-	-	-	-	-	-	-	G	F	D
	C15	S	S	S	S	-	-	L	I	F	S	Y	S	S	I	S	I	S	S	S	S	G	S	T	S	R	Y	H	W	W	Y	Y	Y	P	Y	K	Y	P	A	-	-	-	-	A	F	D
	C16	S	G	Y	E	-	-	P	I	L	Y	S	S	Y	I	S	I	Y	S	Y	Y	G	S	T	Y	R	H	E	T	Y	W	F	S	P	S	-	-	-	-	-	-	-	-	A	M	D
	C17	A	W	Y	S	H	-	P	L	F	S	Y	Y	S	I	S	I	S	S	Y	S	G	Y	T	S	R	I	F	H	Y	R	G	R	Y	S	Y	S	Y	G	Y	-	-	-	A	F	D
	C18	S	S	S	S	-	-	L	I	V	S	Y	Y	S	I	S	I	S	S	S	S	G	S	T	S	R	S	Y	W	Y	Y	I	W	S	Y	S	Y	G	N	-	-	-	-	A	M	D
	C19	G	W	M	R	W	-	P	I	I	S	Y	S	S	I	S	I	Y	P	S	Y	G	S	T	S	R	G	S	S	L	G	S	Y	Y	W	S	A	F	Y	S	-	-	-	G	L	D
	C20	V	M	Y	H	-	-	P	V	I	S	Y	S	S	I	S	I	S	S	S	Y	S	Y	T	S	R	S	Y	I	Y	H	Y	H	Y	G	Y	P	-	-	-	-	-	-	A	F	D
	C21	S	S	W	G	Y	Y	P	V	V	S	Y	S	S	I	Y	I	S	S	Y	S	G	Y	T	S	R	P	Y	V	G	Q	G	K	W	R	Y	Y	S	-	-	-	-	-	A	L	D
	C22	S	S	S	S	-	-	L	I	L	S	S	S	Y	I	S	I	S	S	S	S	G	S	T	S	R	S	G	K	G	G	P	Y	K	W	Y	S	Y	M	F	-	-	-	G	L	D

Figure S2. Sequences of unique sABs generated against *Mj*0480 and CorA. (Related to Figure 2) Bacteria cultures were infected with phage particles harboring sABs with ELISA binding signal A_{450} higher than 0.2 (4 times the average background level in this assay). Subsequently, DNA was isolated from single colonies and sequenced with primers for light and heavy chain to determine the composition of 4 complementarity determining regions (CDRs;

CDR-L3, CDR-H1, CDR-H2 and CDR-H3) randomized in Library E. The sequence of the template of Library E is labeled as 'Library'. Unique sABs clones come from library sorting experiments against 1) *Mj*0480 in nanodiscs (M1 – M32) and in DDM (F1-F7), 2) CorA in nanodiscs in the absence (C1-C10) and presence of D253K competitor (C7-C22). Note that sAB clones C7-C10 appeared in library sorting performed both in the presence and absence of D253K competitor. Numbering of CDRs is according to Kabat.

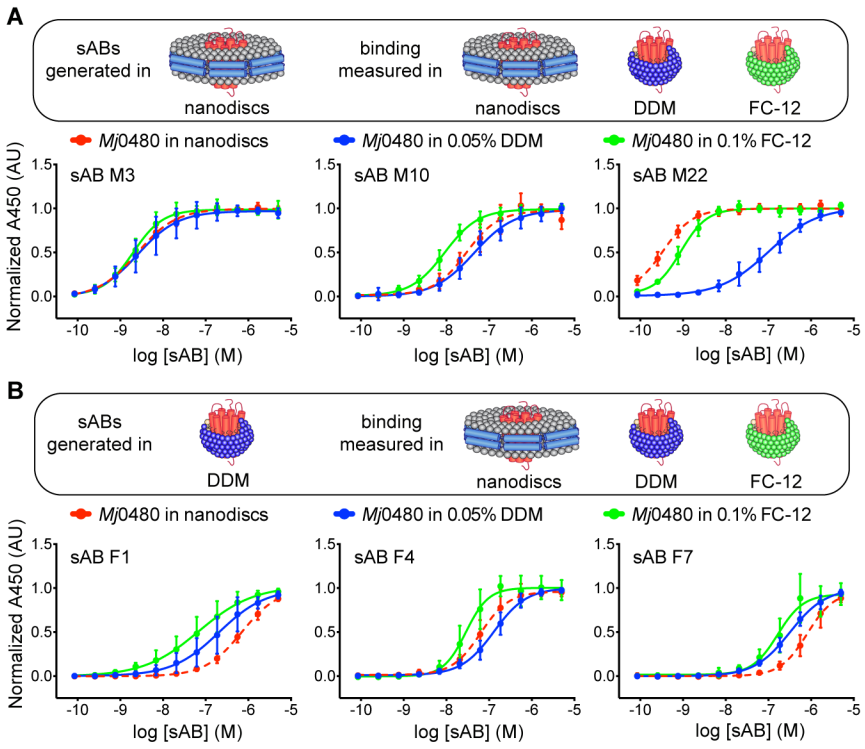

Figure S3. Effect of detergents on binding affinity of additional sABs specific to *Mj*0480 generated in nanodiscs and DDM. (Related to Figure 3) (A)(B) EC_{50} evaluation of apparent binding affinities of *Mj*0480 sABs generated against the antigen in nanodiscs (A) and DDM (B). All sABs in protein format were tested for binding with biotinylated *Mj*0480 in 0.05% DDM (blue, solid), 0.1% FC-12 (green, solid), or *Mj*0480 in biotinylated eggPC E3D1 nanodiscs (red, dashed). Data points in (A) and (B) show average values from 3 independent experiments in triplicates. Error bars display SD value from the mean.

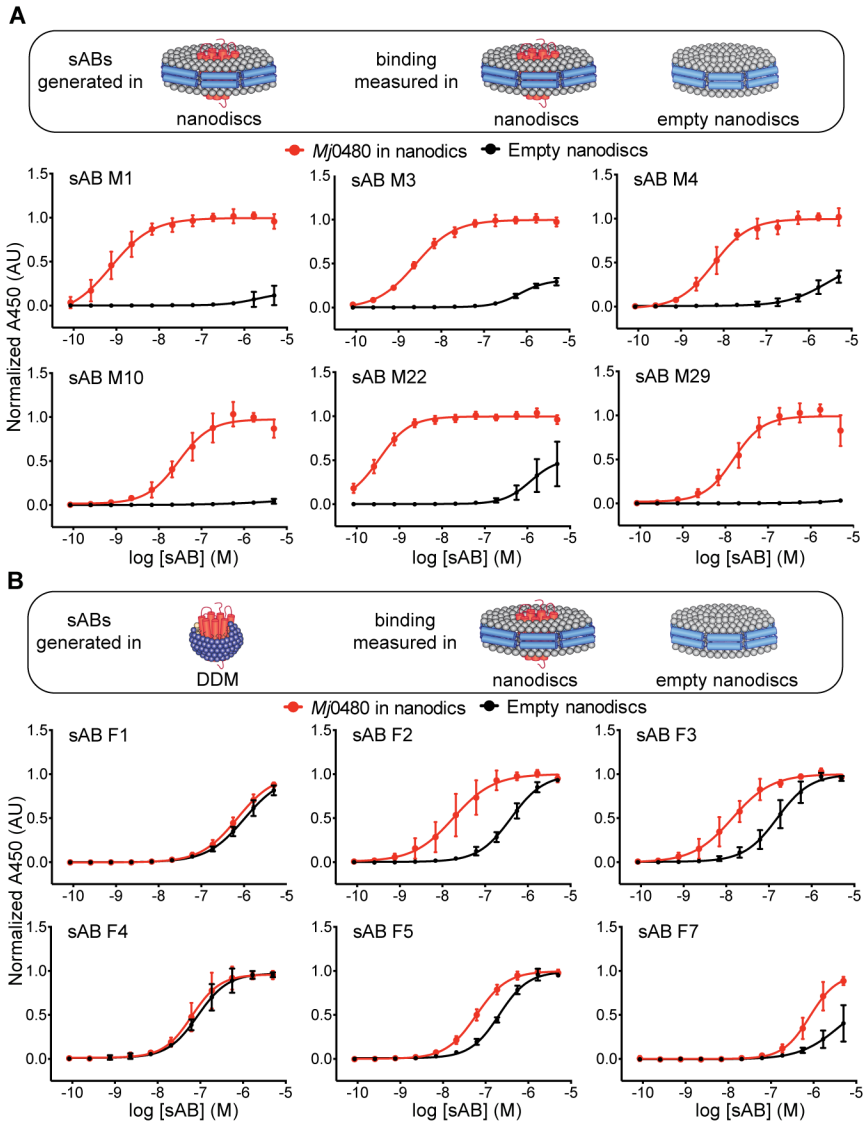

Figure S4. Non-specific binding component of *Mj*0480 sABs generated in nanodiscs and DDM. (Related to Figure 3) (A)(B) EC_{50} evaluation of apparent binding affinities of *Mj*0480 sABs generated against the antigen in nanodiscs (A) and DDM (B). All sABs in protein format were tested for binding with biotinylated nanodiscs loaded with *Mj*0480 (red) or empty nanodiscs (black). Data points in (A) and (B) show average values from 3 independent experiments in triplicates. Error bars display SD value from the mean.

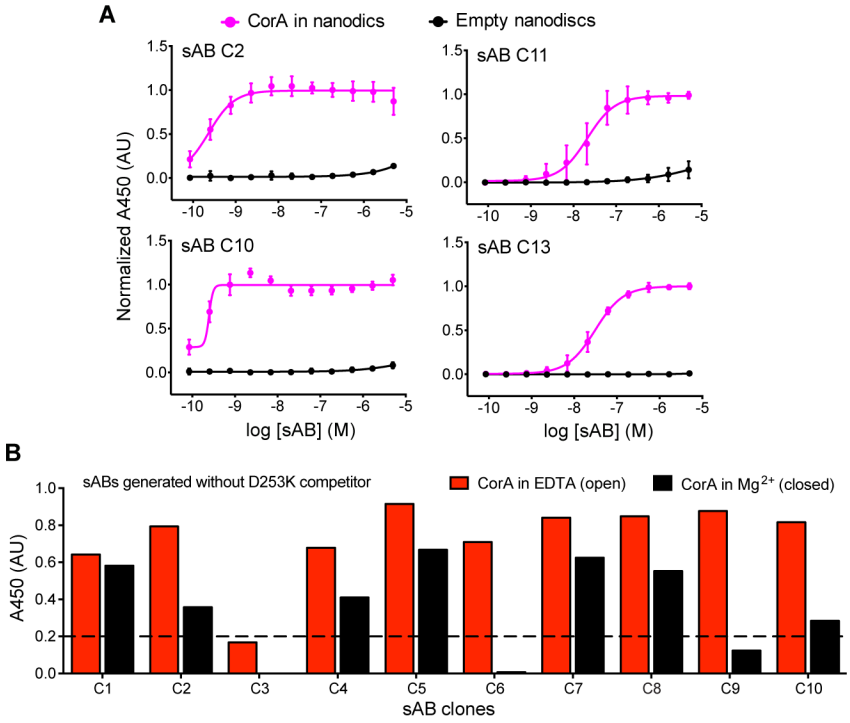

Figure S5. Conformation-specific sABs of CorA – additional analysis. (Related to Figure 4) (A) EC_{50} evaluation of apparent binding affinities of sABs in protein format generated against CorA without (sABs C2 and C10) and with D253K competitor (sABs C10, C11 and C13). In all cases, sABs show low nanomolar apparent binding affinity to CorA in nanodiscs (magenta), but not to empty nanodiscs (black). Data points show average values from 3 independent experiments in triplicates. Error bars display SD value from the mean. See also Figure 2. (B) Representative binding signal of sABs C1-C10 in phage format, generated against CorA wild-type after 5 rounds of library sorting without CorA D253K competitor in nanodiscs. Multiple sABs show high binding signal for biotinylated CorA in nanodiscs in the presence of 1 mM EDTA (open state, red) versus 20 mM $MgCl_2$ (closed state, black). Dotted horizontal line represents 4 times the average background level.

SUPPLEMENTAL TABLES

Supplemental Table S1. Summary of conditions and protein target concentrations during library sorting experiments with *Mj*0480 and CorA in nanodiscs and DDM. (Related to Experimental Procedures; Phage library sorting)

Protein target	***Mj*0480**	***Mj*0480**	***Mj*0480**	**CorA**	**CorA + D253K**[1]
Sorting environment	eggPC[2] E3D1 nanodiscs	DMPC E3D1 nanodiscs	DDM	POPC/POPG E3D1 nanodiscs	POPC/POPG E3D1 nanodiscs
Sorting round	**Concentration of membrane protein in nanodiscs or detergent (nM)**				
1st	400	280	930	220[3]	220[3]
2nd	100	140	460	110	110
3rd	50	85	180	65	65
4th	50	85	90	65	65
5th	10	30	20	20	20

[1]Library sorting with soluble competitor in E3D1 nanodiscs, CorA D253K.

[2]Phosphatidylcholine from chicken egg (Avanti).

[3]Single first round was performed for both library sorting experiments with CorA in E3D1 nanodiscs.

SUPPLEMENTAL EXPERIMENTAL PROCEDURES

Preparation of phospholipids

Phospholipids dissolved in chloroform were dried in glass vials under nitrogen gas. Residual chloroform was successively removed by overnight incubation under vacuum desiccator. Lipids were then dissolved in buffer A (50 mM Hepes pH 7.5, 200 mM NaCl) supplemented with detergent as specified below, and sonicated until clear using digital sonifcator (Branson) with tapered micro-tip. Mixed lipid-detergent micelles were stored at -80 °C and thawed directly before reconstitution of nanodiscs. Stocks of mixed micelles were prepared from the following lipids: egg phosphatidylcholine (eggPC, Avanti), 1,2-dimyristoyl-*sn*-glycero-3-phosphocholine (DMPC, Avanti), palmitoyloleoylphosphatidylcholine (POPC, Avanti), palmitoyloleoylphosphatidylglycerol (POPG, Avanti), and the following detergents: n-dodecyl-beta-D-maltoside (DDM, Affymetrix), and n-undecyl-beta-D-maltoside (UDM, Affymetrix). Mixed micelles used for reconstitution in nanodiscs were composed of: 1) eggPC:UDM (10 mM:20 mM), 2) DMPC:DDM (12 mM:30 mM), and 3) (POPC/POPG):DDM ([9 mM/3 mM]:35 mM).

Nanodisc reconstitution

The nanodiscs were assembled using the following molar ratios of target protein, mixed micelles, and MSP1 E3D1: 1) *Mj*0480:E3D1:eggPC at 1:10:650, 2) *Mj*0480:E3D1:DMPC at 4:10:1200, 3) CorA_wild-type:E3D1:(POPC/POPG) at 5:10:900, and 4) CorA_D253K:E3D1:(POPC/POPG) at 5:10:900. All components were mixed together in a buffer A and incubated on ice for 30 minutes. Next, 400-500 mg activated Bio-Beads SM-2 Adsorbents (Bio-Rad) were added per each ml of assembly mix (Bio-Beads were activated by incubation in methanol and successively washed with copious amounts of water); the reconstitution reaction was left shaking overnight at 4 °C. Supernatant was collected in a fresh tube, and then hard spun at 15,000 x g at 4 °C for 10 min. Nanodisc suspensions were then incubated with Ni-NTA Superflow resin (Qiagen, 500 ul of resin per 1 ml of assembly reaction) for 1 h at 4 °C on a shaker to remove empty nanodiscs. For empty nanodiscs assembled for the purposes of competitive library sorting, this step was omitted. Nanodiscs with embedded membrane proteins were eluted from the resin using buffer A supplemented with 300 mM imidazole. Eluted fractions containing nanodiscs were concentrated to 500 µl and injected onto Superdex 10/300 GL (GE Healthcare) column in

the buffer A. Each nanodisc preparation was run alongside an empty nanodisc control. The collected fractions were evaluated by SDS-PAGE, and peak fractions containing both MSP1 E3D1 and the target membrane protein were collected for further experiments.

Library sorting

Round 1 of sorting was performed manually using membrane protein antigens (biotinylated in nanodiscs or detergent) bound to streptavidin-coated magnetic beads. Upon antigen binding, the beads were washed in buffer B (1% BSA in buffer A), supplemented with either 1 mM EDTA (buffer C) for sorting with CorA-wt, or 0.05% DDM (buffer D) for sorting with *Mj*0480 in detergent. Beads were subsequently blocked with 5 μM biotin, and exposed to the phage library in buffer B, C or D for 1 hour at room temperature with shaking. Beads were then washed with buffer B, C or D to remove non-specific phage particles, and used to infect log phase *E. coli* XL-1 strain (Stratagene). Cells were grown in 2xYT media (Fisher) supplemented with 50 μg/ml ampicillin and 10^9 pfu/ml of KO7 helper phage (NEB) overnight at 37 °C and 280 rpm to amplify the phage particles. The amplified phage particles after round 1 were subsequently used in four additional rounds of library sorting performed semi-automatically with a KingFisher magnetic bead handler (Thermo) according to described protocols (Fellouse et al., 2007). Starting from round 2, the amount of biotinylated antigen immobilized on magnetic beads was decreased to achieve increasing selection pressure during phage library sorting. Such selection pressure varied depending on the round, membrane protein, and the number of amplified phage particles from the previous round; the concentrations of antigen used in library sorting are summarized in Supplemental Table S1.

Starting from round 2, in every step except elution, the buffer was supplemented with at least 5- to 10-fold molar excess of non-biotinylated empty nanodiscs assembled from the same lipid stock as the biotinylated nanodiscs with antigen to counter-select for MSP-, lipid-, and non-specific phage particles. Finally, in each of rounds 2-5, phage particles were eluted from magnetic beads by 15-minutes incubation with either 1% Fos-Choline-12 or 0.05% DTT in buffer B. For library sorting with wild-type CorA in nanodiscs, starting from round 2, an additional library sorting was performed where, as a soluble competitor, 10-fold molar excess of CorA D253K (a closed variant of CorA) was used to further push the sorting pressure towards phage particles with sABs specifically recognizing the open conformation of CorA. In round 4,

input phage particles were tested in two concurrent sorting experiments: one with antigen-embedded biotinylated nanodiscs, and one with empty magnetic beads, to directly compare the amount of phage particles specifically retained by the biotinylated sample (to assess so-called 'enrichment' levels). In round 5, for each input phage the enrichment was additionally tested with sorting against biotinylated empty nanodiscs of the same chemical makeup as the membrane protein antigen to evaluate the number of phage particles specific for the membrane protein. For library sorting with *Mj*0480 in DDM, the enrichment level in rounds 4-5 was tested on empty magnetic beads only.